Nanoscale

Accepted Manuscript

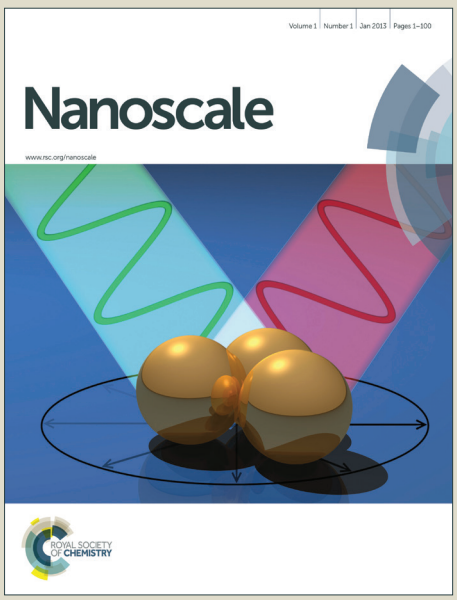

ROYAL SOCIETY OF CHEMISTRY

www.rsc.org/nanoscale

Nanoscale

Review

Recent Advances in Noble Metal Based Composite Nanocatalysts: Colloidal Synthesis, Properties, and Catalytic Applications

Received 00th January 20xx,
Accepted 00th January 20xx

DOI: 10.1039/x0xx00000x

www.rsc.org/

Yong Xu[a, #], Lei Chen[a,#], Xuchun Wang[a], Weitang Yao[b,*], Qiao Zhang[a,*]

This Review article provides a progress report on the synthesis, properties and catalytic applications of noble metal based composite nanomaterials. We begin with a brief discussion on the category of various composite materials. We then present some important colloidal synthetic approaches to the composite nanostructures, in which major attention has been paid to the bimetallic nanoparticles. We also introduce some important physiochemical properties that are beneficial from the composite nanomaterials. Finally, we highlight the catalytic applications of such composite nanoparticles, and conclude with remarks on prospective future directions.

1. Introduction

Catalysis is of fundamental importance to the chemical industry. The ultimate goal of catalysis research is to understand the catalytic process at the molecular level and design catalysts with desired activity and selectivity.[1] With the development of nanotechnology over the past several decades, it is widely accepted that nanoparticles tend to show better catalytic performance than their bulk counterpart because of their smaller particle size as well as the "nano-effect" originated from the small size. As a result, many synthetic methods have been developed in order to prepare nanoparticles with controllable morphologies and narrow size distribution. For example, noble metal nanoparticles (Au, Ag, Pd, Pt *et al.*) have received increasing interest due to their unique physiochemical properties and their potential applications in various fields, such as biomedicine,[2-4] sensing,[2, 5] surface-enhanced Raman scattering (SERS),[6, 7] photothermal therapy,[4, 8, 9] and especially catalysis[10-16]. To date, researchers are able to synthesize noble metal nanoparticles with various shapes and controllable dimensions, including zero-dimensional,[17-19] one-dimensional,[20-24] two-dimensional,[25-29] and three-dimensional nanoparticles,[30, 31] in an elegant manner. And one can tailor the properties of noble-metal nanostructures and thus improve their performance in catalysis by controlling their size, shape, composition, and interfacial interactions.[13, 32]

Recently, it is gradually realized that a single-component material usually does not meet all the requirements in terms of high activity, high stability, high selectivity, *etc*. On the other hand, more and more attention has been paid to composite nanomaterials that made of two or more components. Because the composite nanomaterials combine the functions of individual component and can overcome the limitation of single component in catalytic application.[33, 34] Among various composite catalysts, bimetallic catalysts have gained much attention and have been widely used in many applications.[35] For instance, bimetallic catalysts have been widely used for the oxidation, hydrogenation, hydrogenolysis and reforming reactions.[35] Recently, the applications of composite catalysts have been extended to biomass chemical industry which is regarded as a promising supplement to the petroleum industry.[36, 37] Up to now, the synthesis of composite nanocatalysts with tailored morphologies and tunable compositions has been achieved via diverse approaches, leading to a significant progress in nanocatalysis during the past decades.[38-51]

Based on different mixing patterns, composite catalysts can be roughly divided into three major categories: core-shell nanostructures, heterostructures, and alloyed nanostructures, as shown in Figure 1. There are many sub-groups under each major category. For example, there are four general components that can be engineered to prepare various core-shell nanostructures.[52] First, regarding the overall architecture, one can prepare concentric yolk-shell nanostructures or anisotropic structures. Second, by tuning the number as well as the components of the core particle, one can prepare core-shell nanostructures with either single-core or multi-core or multi-component core. Third, by engineering the shell nanostructure, we can obtain core-shell nanostructures with single-shell or multi-shell or porous shell. Finally, by tuning the interface, one can synthesize core-shell nanostructures with different interfacial properties, which is critical for the development of nanocatalysts with improved performance. Because there are so many different types of composite nanostructures, we are not going to describe too much detail on the sub-groups of each major category.

[a] *Jiangsu Key Laboratory for Carbon-Based Functional Materials & Devices, Institute of Functional Nano and Soft Materials (FUNSOM) and Collaborative Innovation Center of Suzhou Nano Science and Technology, Soochow University, Suzhou 215123, P. R. China*
[b] *Joint Laboratory for Extreme Conditions Matter Properties， Southwest University of Science and Technology, Mianyang, Sichuan 621010, China*
[#] *These authors contribute equally to this work.*

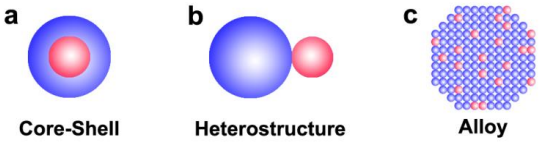

Figure 1. Schematic illustration of three major categories of noble-metal based composite nanomaterials: (a) core-shell nanostructures; (b) heterostructures; and (c) alloyed nanostructures.

In this review article, we seek to describe and discuss recent advances in the synthesis, properties and applications of noble metal based composite nanocatalysts. We will first review the recent advances in the synthesis of noble metal nanocomposites. Major emphasis will be put on the colloidal synthesis of bimetallic nanostructures. Then, we will focus on some unique physiochemical properties of the nanocomposites, especially the plasmonic and catalytic properties. At last, the promising catalytic application of noble metal based nanocomposites are presented with an emphasis on bimetallic, tri-metallic, and metal-oxide composites.

2. Colloidal Synthesis

The synthesis of noble metal based composite nanocatalysts is generally more complicated than mono-metallic catalysts. In order to obtain composite catalysts with desired structures as well as desired properties, many factors should be taken into consideration, including crystal structure of each component, the relative strength of the bond among different elements, surface energy, relative atomic sizes, capping ligand, electronic effects, and so forth.[53] During the past two decades, the synthesis of composite catalysts has attracted great attention. Hundreds of papers are published in this field every year. Composite nanomaterials can now be prepared via various approaches, including colloidal synthesis, CVD method, atomic layer deposition (ALD) method, electrochemical approach, and so on. In this Review article, we will mainly focus on the colloidal synthesis of composite nanostructures. Our major attention will be paid to the bimetallic nanostructure systems. Less attention will be paid to metal-oxide or metal-salt systems.

Chemical reduction method Noble metal nanoparticles are generally obtained by chemical reduction method in the presence of an appropriate surfactant (*e.g.*, citrate) or polymeric ligands (*e.g.*, polyvinylpyrrolidone, PVP) that can passivate the surface of nanoparticles and prevent them from aggregation.[5, 54-57] Although the procedure for synthesizing composite nanoparticles using chemical reduction method is similar with that for mono-metallic nanoparticles, it is more difficult to control the co-reduction process of mixed metal ions because of the difference in the reduction potentials and inherent chemical nature. In general, simultaneous reduction processes were used to prepare alloyed composite metal nanostructures, while sequential reduction processes were used to prepare core-shell nanostructured composites. Therefore, a suitable reducing agent is critical for obtaining the controllable composite nanoparticles.

Sodium borohydride ($NaBH_4$) is a strong reducing agent that can enable a rapid nucleation and growth of noble metal nanoparticles, and has been widely used for preparing the composite catalysts.[58-] Wang and co-workers reported a protocol for generatin monodispersed Cu-Pt and Cu-Au composite nanoparticles, in whic metallic ions could be reduced sequentially by $NaBH_4$ to form nanocomposites.[63] However, strong reducing agents can general cause a quick and less controllable reduction of metal ions. To get better control over the reaction kinetics as well as the produc some mild reducing agents, such as ethylene glycol and diethylene glycol (also called polyol process),[64] citrate/sodium citrate,[65-] ascorbic acid,[70] formic acid,[71] 2-thiopheneacetonitrile,[72] polymers, and oleylamine,[74, 75] have been used to obtain monodispersed composite nanoparticles in solution. In this condition, a mild reducing agent can rapidly reduce one metal with higher reductio potential that tends to form a core, while the second metal reduced at later stage and deposited on the surface of the cor thus to form the core-shell nanostructure. For example, nobl metals ions (*e.g.*, Pt) can be effectively reduced by a mild redu agent (*i.e.*, octadecylamine) first, while the transition metal ions (*e.g.*, Ni, Zn, Co, Cd and In) will be reduced later due to their lo reduction potentials. Li and co-workers have done excellent work in preparing these composite nanoparticles.[76, 77] By using method, many noble metal based composite nanoparticles wit different nanostructures have been synthesized, including Cu-Pt Co-Pt, Ni-Pt, In-Pd, Zn-Pt and In-Pt nanocomposites (Figure 2).[77]

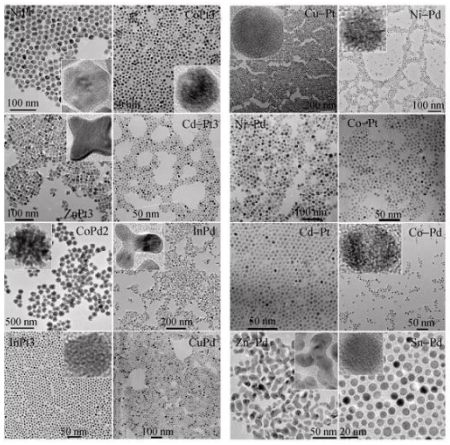

Figure 2. TEM images of noble metal based composite catalyst (Ni-Pt, Co-Pt, Cu-Pt, Ni-Pd, Zn-Pd, Cd-Pd, Co-Pd, In-Pd, In-Pt and Sn-Pd). Reproduced with permission from ref. [77]. Copyright 201 Springer.

Hydrogen can also be used as a mild reducing agent when the composite catalysts are prepared by co-precipitation impregnation.[78-80] For synthesizing the composite catalysts, supporter with large surface area (*e.g.*, Al_2O_3, SiO_2 and zeolites *etc* is usually needed. The noble metal precursors are directly deposited on the supporter, followed by a further calcination fo the thermolysis of metal precursors to form metal oxides. And the hydrogen is used to reduce the oxides to obtain the supported catalysts. For example, Su and co-worker have prepared Pd/A bimetallic catalysts supported on the mesoporous silica nanoparticles (MSN) by an impregnation approach. The activ

noble metallic components reduced by hydrogen are highly dispersed on MSN with a tunable molar ratio from 0.1 to 0.4 (Figure 3).

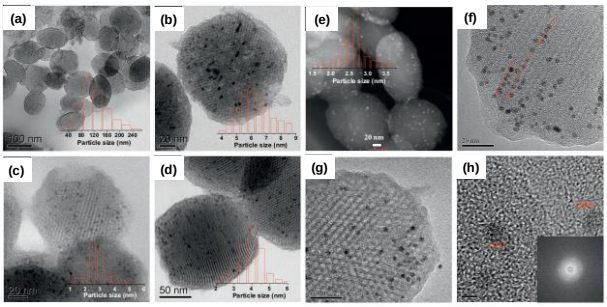

Figure 3. HRTEM images of (a) MSN, (b) Pd/MSN, (c) $PdAu_{0.1}$/MSN, and (d) $PdAu_{0.4}$/MSN catalysts. STEM (e) and HRTEM (f-h) images, with corresponding electron diffraction pattern (inset in h) of the optimized $PdAu_{0.2}$/MSN. Reproduced with permission from ref.79. Copyright 2012, Elsevier Inc.

Thermal decomposition method The decomposition of a mixture of organometallic compounds or labile noble-metal salts at elevated temperature is a widely used approach to synthesize noble metal based composites.[81-83] This approach is usually conducted in non-aqueous media under inert atmosphere. Compared to aqueous synthesis of bimetallic nanoparticles that conducted in water, this method has some advantages, such as narrower size distribution and more tunable compositions of product. For example, noble metal nanostructures can be combined with a lot of transition metals, which is usually not available in the aqueous phase synthesis.[84-86] In addition, introducing a small amount of oxygen into the prepared bimetallic nanoparticles can be used to make metal-metal oxide composites.

Sun *et al.* have prepared monodispersed Fe-Pt composite nanoparticles from the precursors of $Pt(acac)_2$ and $Fe(CO)_5$ through thermal decomposition method in the presence of oleic acid and oleylamine.[87] The ratio of Fe and Pt in the composite nanoparticles can be systematically tuned by altering the concentration of $Pt(acac)_2$ and $Fe(CO)_5$. Thomas and co-workers have synthesized bimetallic nanoparticles of Ru-Pd, Ru-Sn, Ru-Pt, Ru-Cu, and Ru-Ag by the decomposition of organometallic clusters at around 200 ^{o}C for 2 h in vacuum.[81] Bronstein's group has synthesized Pt-Fe nanoparticles by using a two-step process, in which the iron nanoparticles were pre-synthesized *via* a thermal decomposition at 200 ^{o}C, followed by a second thermolysis of $Pt(acac)_2$ in the presence of oleic acid and oleylamine at 285 ^{o}C. The two phases of Pt and Fe in obtained nanoparticles are composited in the manner of side by side (Figure 4).[88] Pan *et al.*, synthesized carbon supported Pd-Fe composite nanoparticles with small particle size and the single-phase *fcc* disordered structure using the precursors of $Pd(CH_3COO)_2$ and $Fe(CH_3COO)_2$ in the absence of additional stabilizers, giving an excellent electrocatalytic activity for the oxygen reduction reactions (ORR).[84] This method has been extended to use other precursors including $PdCl_2$ [86, 89] and $[Pd(NH_3)_4](NO_3)_2$ [85, 90] to generate Pd-based composite catalysts.

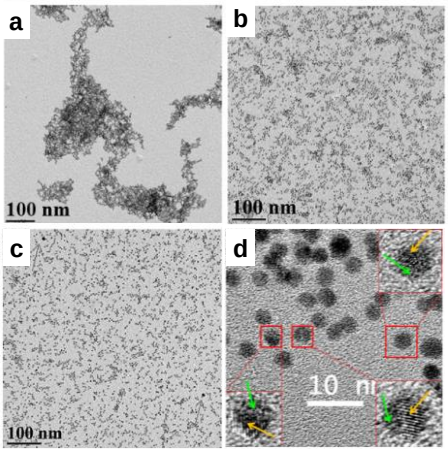

Figure 4. TEM images of (a) Pt-Fe_3, (b) Pt-Fe_2, (c) Pt-Fe_1, and (d) HRTEM images of the Pt-Fe_3 sample. The three insets show zoomed-in views of individual NPs. Yellow and green arrows indicate different domains in a single particle. Reproduced with permission from ref. 88. Copyright 2014, American Chemical Society.

In addition, the thermal decomposition method has also been used to synthesize Au-based [89] and Ag-based [91] composite nanoparticles. Lee's group has recently synthesized the Ag-Cu bimetallic nanoparticles through a two-step process.[91] Cu(acac)$_2$ was thermally decomposed at 220 ^{o}C to form Cu nanoparticles in the presence of oleylamine. $AgNO_3$ was subsequently added and was further reduced by Cu through the galvanic displacement reaction. Highly monodispersed Ag-Cu composite nanoparticles with a narrow size distribution were obtained, giving a decreased O_2 adsorption energy comparing with pure Cu (Figure 5).

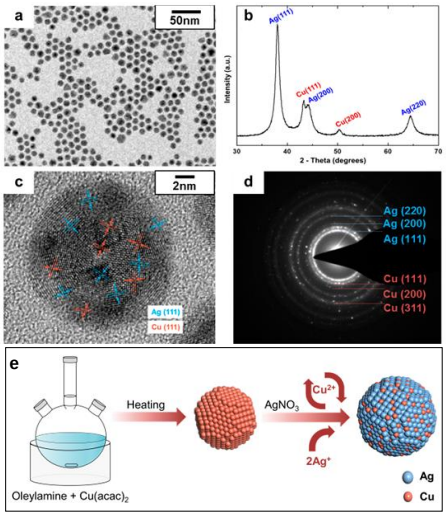

Figure 5. (a) TEM image of the Ag-Cu nanoparticles synthesized at 220°C for 2 h (initial Cu nanoparticle nucleation and growth) and 180°C for 6 h. (b) Characterization by XRD of the synthesized Ag-Cu nanoparticles. (c) HRTEM image of a nanoparticle. (d) SAED pattern of the Ag-Cu nanoparticles. (e) Schematic illustration of the synthesis of Ag-Cu nanoparticles. Galvanic displacement and reduction of Cu occur due to the difference in Ag and Cu redox potentials and oleylamine-based thermal decomposition

respectively. Reproduced with permission from ref. 91. Copyright 2014, American Chemical Society.

Biosynthesis method Biosynthesis methods have been suggested as promising alternative synthetic routes for synthesizing nanoparticles because they do not require additional chemical reagents or complex experimental apparatus. At the beginning, people are trying to utilize the biomass extracts as the reducing agent as well as the capping ligand to prepare metallic nanocomposites.[92] Li group used *Cacumen Platycladi* leaf extract as reducing agent to synthesize Au-Pd[93, 94] and Au-Ag[95, 96] composite nanoparticles. The composition and particle size of the obtained nanoparticles were determined by the concentration of *Cacumen Platycladi* leaf extract.[95] Recently, other biomass extracts, including mahogany leaves,[97] micro-alga,[98] Neem (*azadirachta indica*) leaf,[99] *piper pedicellatum* C.DC,[100] *Fusarium oxysporum*,[101] and chloroplasts,[102] have been explored to synthesize noble metal based composite nanoparticles. Besides, microorganisms have also been used for synthesizing the noble metal based composite nanoparticles. Avalos and co-workers have reported a biosynthetic method for the production of Ag-Au composite nanoparticles by using the fungus *N. crassa*. It is found that the size and composition of the composite nanoparticles can be controlled by the fungus.[103]

Biomimetic synthesis is another important route for obtaining nanostructures.[104] Numerous biological systems, such as proteins [104-108] and DNA,[109-111] have been used to direct the growth of noble metal based composite nanoparticles. For example, Monika *et al*. reported that uniform and size-tunable bimetallic Ag-Au nanowires can be obtained by using artificial DNA templates *via* a two-step metallization process.[111] Rotello and co-workers have synthesized Fe-Pt composite nanoparticles through DNA-mediated ''bricks and mortar'' self-assembly process. It is reported that the magnetic properties of the assemblies can be altered by the enhanced structure and increased spacing in the bio-nanocomposite assembly.[112] Additionally, virus is considered as an attractive template for constructing and organizing the nanostructure, because it has the capabilities of molecular recognition and self-assembly.[113, 114] Belcher and co-workers have reported the synthesis and self-assembly of Au-Co_3O_4 and Au-Ag nanowires using virus. The synthesis and self-assembly of nanoparticles have shed light on the development of lithium ion battery (Figure 6).[115, 116]

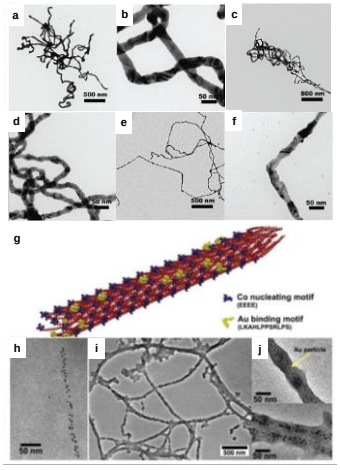

Figure 6. Characterization of CTAB-stabilized Au_xAg_{1-x} alloy nanowires on p8#9 virus. (a, b) TEM images of $Au_{0.9}Ag_{0.1}$ nanowires, (c, d) TEM images of $Au_{0.67}Ag_{0.33}$ nanowires, and (e, f) TEM images of $Au_{0.5}Ag_{0.5}$ nanowires. Reproduced with permission from ref.[115] Copyright 2010, American Chemical Society. (g) Visualization of the genetically engineered M13 bacteriophage viruses. P8 proteins containing a gold-binding motif (yellow) were doped by the phagemid method in E4 clones, which can grow Co_3O_4, (h) TEM images of the assembled gold nanoparticles on the virus, (i, j) TEM image of hybrid nanowires of Au nanoparticles/Co_3O_4. Reproduced and adopted with permission from ref. 116. Copyright 2006 American Association for the Advancement of Science.

Galvanic replacement Galvanic replacement is an electrochemical process, in which a preformed metal nanoparticle can be oxidized by the ions of another metal that has a relatively higher reduction potential. In this process, the preformed nanoparticle can be regarded as a sacrificial template which will be dissolved into the solution, and the second metal will be deposited onto the outer surface of the template. As a result, the final product usually possesses a shape similar to that of the template. But different from solid templates, the product is featured with porous outer shell and hollow interior. By carefully controlling parameters of the redox reaction process, composite nanomaterials with different composition and various shapes can be obtained.

The first report on the nanoscale galvanic replacement was done by the Xia group in 2002, in which they prepared hollow gold nanostructures using silver nanoparticles as the sacrificial templates.[117] Since then, galvanic replacement method has been widely used to prepare various composite metallic nanostructures including Au-Ag, Au-Cu, Pd-Pt, Ag-Pt, Ag-Pd, *etc*.[118-122]

Sonochemical method Sonolysis of water can generate H· radicals, which are considered to act as reducing agent to reduce metal ions. The sonochemical reduction method has been widely used to synthesize bimetallic nanomaterials.[123] Compared with other traditional chemical reduction methods, this method has several advantages. First, no chemical reducing agent is needed. Second, the reaction rates are reasonably fast. And third, very small metal particles can be produced because of the high reaction rate.[124] Although a lot of mono-metal nanoparticles (*e.g.*, Au, Ag, Pt, and Pd) have been prepared through this approach,[125-127] few

reports that make bimetallic nanoparticles have been found. The pioneering contributions were reported by Mizokoshi and co-workers, who have prepared Au-Pd bimetallic nanoparticles and Au@Pd core-shell nanostructure by using sonochemical method.[128, 129] In the subsequent publications, some other noble metal based composite nanoparticles, including Pd-Cu,[130] Pt-Sn,[131] Pt-Co,[132] Pt-Pd,[133] Au-Ag,[134] and Ag-Pd,[135] have been synthesized by using sonochemical methods.

Radiolysis method In this method, metallic ions are reduced by solvated electrons irradiate by γ-ray radiation. The γ-ray determines the rate of reduction and hence the final structure of composite nanoparticles. Radiolysis is an efficient method for reducing metal ions to obtain noble metal based composite nanoparticles, including Ag-Au,[136] Cu-Ag,[137] Pd-Ag,[138] Pt-Ag,[139, 140] Ag-Tl,[141] Pd-Al,[142] Pd-Au,[143-146] Pt-Au,[143, 147] Au-Ni,[148] and Cu-Pt[149] nanoalloys.

3. Properties

A unique and attractive feature of composite nanoparticle is that one can integrate multi-functions into one single unit or even create some properties that cannot be obtained by simply mixing different components. In this part, we will highlight some interesting properties, including surface plasmon resonance, magnetic, and catalytic properties, that are beneficial for the catalytic applications.

Surface plasmon resonance (SPR) properties

Studies on the optical properties of noble metal nanoparticles can be dated to 1857 when Michael Faraday prepared various gold colloids with different colors. We now understand that the different colors are caused by surface plasmon resonance (SPR), which occurs when a metallic nanoparticle of appropriate size interacts with incident photons in such a way as to confine the resonant photon within the dimensions of the nanoparticles.[150] These unique optical properties have inspired promising applications of noble metal nanoparticles. To better understand the plasmonic properties, some theories or methods have been proposed to simulate the collective excitation of electrons in metallic particles, including Mie theory,[151] discrete dipole approximation (DDA),[152] boundary element method (BEM),[153] T-matrix, [154] and finite differences in the time domain (FDTD). [155-159] Gold and silver nanoparticles are the most widely studied noble metal nanoparticles for investigating optical properties of metallic composite nanoparticles, because their SPR peaks are located in the visible region.[49,160, 161] It is well known that the SPR peak of nanoparticles is highly dependent on their shape, composition, and architecture.

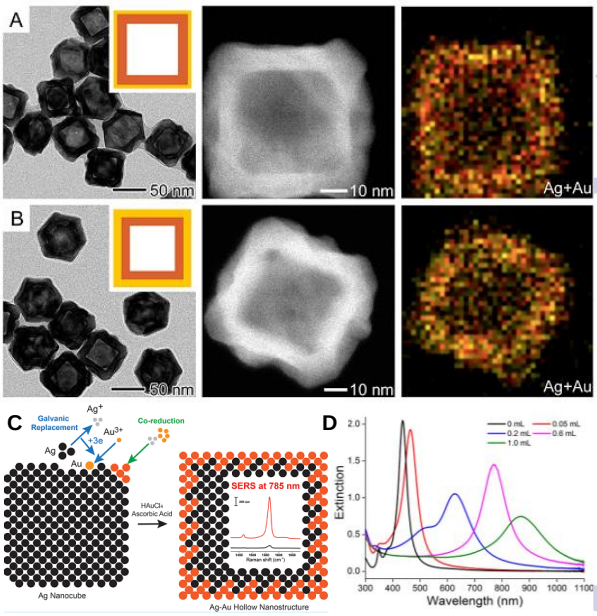

Figure 7. TEM images, illustrations (insets), HAADF-STEM ima[ges] and EDX mapping analyses of Ag nanocubes after reaction with two different volumes of 0.2 mM aqueous $HAuCl_4$ solution in the absence of ascorbic acid: (A) 1.0 and (B) 1.5 mL. (C) Scheme of th[e] co-reduction of silver nanocube and Au^{3+}. (D) UV-vis-NIR spectra of aqueous suspensions of Ag nanocubes before and after reactin[g] with different volumes of 0.2 mM aqueous $HAuCl_4$ solution in the absence of ascorbic acid. Reproduced with permission from re[f.] 162. Copyright 2014, American Chemical Society.

A critical factor to determine the overall plasmonic properties of composite nanoparticles is the ratio of each component. Fo[r] example, Kim and co-workers have investigated the LSPR properties of individual AgAuAg nanorods using the dark-field spectr[al] microscopy technique. The scattering spectra of such hetero nanorods show longitudinal resonance wavelengths that are near[ly] insensitive to the relative composition of Ag and Au, suggesting that the plasmonic properties are determined by the overall geom[etry] as well as the composition of the hetero-metallic nanostructures.[163] Chen *et al* have investigated the plasmonic properties of the star-shaped Au-Ag bimetallic nanoparticles, in which the SPR wavelength of the composite nanoparticles is strongly depended on the ratio of gold and silver.[164] Yang and co-workers have studied the plasmonic properties of Ag-Au hollow nanocubes prepared through the galvanic reaction between silver nanocubes and $HAuCl_4$, showing that the SPR wavelength of the Ag-Au hollow nanocubes could be tuned by adjusting the addition of gold source (Figure 7).[162]

Recently, it is realized that one can tune the SPR peak by engineering the architecture of composite nanomaterials, *e.g.* core-shell, 3D architectures, *etc.* For instance, the coupling effect between gold and silver nanoparticles can significantly enhance the plasmonic properties, which may be affected by the compositions and structures.[165, 166] For core-shell nanostructures, it has been reported that the outer shell determines the overall character of the optical response. A gold core within a silver shell leads to a distinct red-shift of SPR wavelength. A single outer layer of Ag [...]

produce an Ag-like resonance even in a gold-rich structure.[167-169] To better understand the coupling effect of the core and shell, Donoval and co-workers have calculated the effects of silver shell on the overall plasmonic properties of Au@Ag core-shell nanostructures. Theoretical results indicate that an increasing of silver ratio in the shell leads to a blue-shift of SPR wavelength.[170] Maye's group have investigated the effects of Au-Ag alloy shell on the plasmonic properties of Au@Au-Ag composite nanoparticles, suggesting that the plasmonic properties could be tuned by altering the processing temperature, alloy composition as well as the alloy thickness.[171, 172] In addition, the effects of shell on optical properties have also been proved by Singh and Soni through the preparation of Al@Al_2O_3@Ag@Au core-shell nanostructures with multilayer shells, in which the SPR wavelength could be systematically tuned by altering the composition of Au in nanostructures.[173]

Additionally, it has been reported that metallic dimers and their decoupling from the substrate in a three-dimensional (3-D) design can further improve their SERS performance. Krahne's group recently synthesized 3-D Au-Ag nanostar dimer in ring structures (NSDiR) through electron-beam lithography method. It is demonstrated that the electromagnetic field enhancement is significantly enhanced because of the efficient decoupling from the substrate, indicating that the plasmonic properties can also be affected by the interactions between composite nanoparticles and substrate (Figure 8).[174]

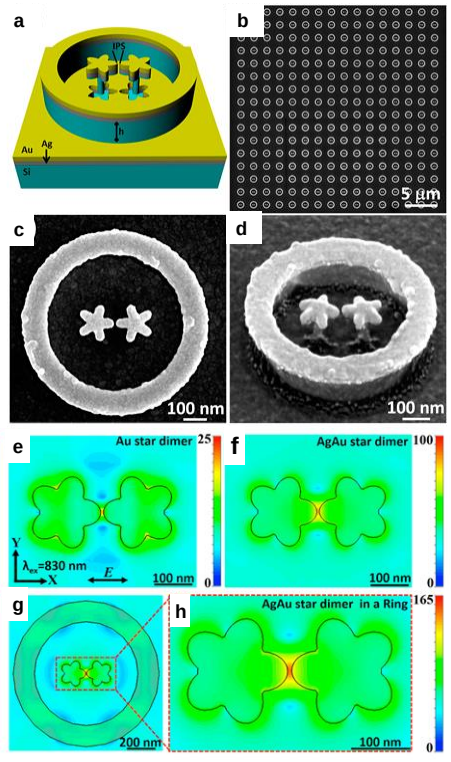

Figure 8. (a) Schematic illustration of a Ag-Au 3D-NSDiR structure. (b) Normal-incidence SEM image of Ag-Au 3D-NSDiR structures. (c-d) Magnified image of a Ag-Au 3D-NSDiR structure with S5 size at normal incidence and at 52° tilted view, respectively. (e-g) Electricfield distribution of a Au nanostar dimer, a AgAu nanostar dimer, and a AgAu nanostar dimer in a ring (3D-NSDiR), respectively, in the *x-y* plane. (h) Magnified view of a 3D-NSDiR from (g). The scale bars represent the field enhancement, with the incoming field E_0 equal to 1. Reproduced with permission from ref 174. Copyright 2014, American Chemical Society.

Investigations on plasmonic properties of noble metal based composite nanoparticles have been extended to a number of noble metal based composite nanoparticles, including: Au-Pd,[175-178] Ag-Pt,[179] Au-Cu,[180-182] Au-Ni,[183] Ag-Cu,[184] Ag-Pd,[178] Cu-Pd,[185] Fe-Pd,[186] and Rh-Pd,[187] which may inspire some promising applications of noble metal based composite nanoparticles.

Magnetic properties

Magnetic metal elements (*e.g.*, Fe, Co, Ni) have two 4s outermost electrons and unsaturated 3d electron shell, which induce rich physicochemical properties, such as specific magnetic and catalytic performances.[188, 189] The combination of noble metals with magnetic metals has shown great scientific significance, since the multifunctional nanostructures may provide some promising physicochemical properties.[190-193] For example, it is well known that magnetic 3d metal clusters exhibit the phenomenon of giant magneto-resistance (GMR) when they are mixed with nonmagnetic metals or even insulators. These GMR materials have shown promising applications in magnetic sensing and recording, resulting in the studies of composite nanoalloys between magnetic 3d metals and nonmagnetic 4d (*e.g.*, Rh, Pd, Ag) or 5d metals (*e.g.*, Pt, Au).[194] The magnetic properties of composite nanoparticles among noble metals and magnetic metals have been widely investigated during the past decades.[194-200] Investigations on the magnetic properties of Fe-Ag composite nanoparticles with different ratios of Fe and Ag including $Fe_{90}Ag_{10}$,[197, 201] $Fe_{75}Ag_{25}$,[197, 202] $Fe_{55}Ag_{45}$,[203] $Fe_{50}Ag_{50}$,[197] $Fe_{35}Ag_{65}$,[204] and $Fe_{25}Ag_{75}$,[197, 204] suggest that the magnetic properties of composite nanoparticles are strongly depended on the interactions between the different elements as well as structural arrangement (Figure 9). The studies of magnetic effects of noble metal based composite nanoparticles have been extended to other systems, such as Fe-Pt,[205, 206] Fe-Pd,[207, 208], Fe-Au,[209, 210] Fe-Ag,[211] Ni-Au,[212] and Ni-Pt.[213]

In addition, the manipulation of magnetic properties can be achieved by controlling the morphologies of composite nanoparticles. The studies of Fe-Au nanorods indicate that the performance of magnetic tweezers and high gradient magnetic separation can be improved by the manipulation of magnetic properties.[214] Other shapes of composite nanoparticles, including core-shell nanostructure,[215-217] nanocat,[218] and sandwich,[219-221] have also been reported for investigating the magnetic properties of noble metal based composite nanoparticles.

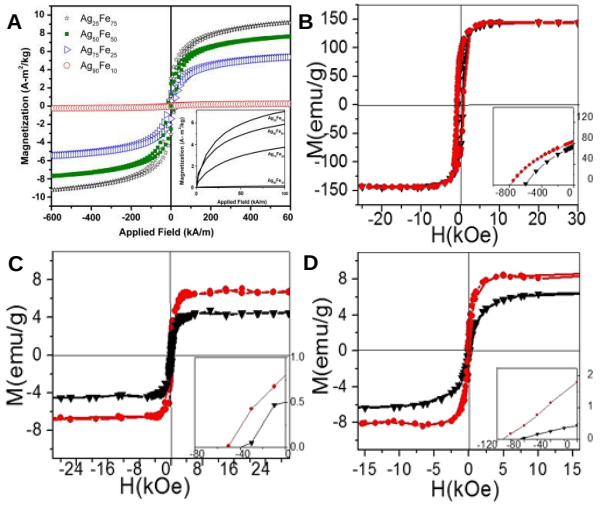

Figure 9. (A) Magnetic hysteresis curves of $Ag_{90}Fe_{10}$, $Ag_{75}Fe_{25}$, $Ag_{50}Fe_{50}$ and $Ag_{25}Fe_{75}$ samples taken at room temperature. The inset shows the samples attaining saturation magnetization at low applied fields. Reproduced with permission from ref.[197]. Copyright 2013, Elsevier B.V. (B-D) Magnetization (M) *vs.* Applied field (H) loops of Au-Fe nanoparticles at 10 and 300 K, compositions 79 (B), 53 (C), and 33 (D) atom % Fe, respectively. The properties at 10 and 300 K are represented by red dots and black triangles, respectively. The insets show second quadrant behaviour. Reproduced with permission from ref. 210. Copyright 2014 American Chemical Society.

Catalytic properties

Noble metal nanoparticles have been widely used in catalysis due to their unique catalytic performance.[222-224] However, the application of monometallic noble metal catalysts have been seriously impeded by several factors, including high cost, low stability, low selectivity, *etc*. It is realized that the catalytic performance of noble metal nanoparticles can be significantly improved by incorporating some other components to form composite nanostructures. The composite nanoparticles can potentially achieve the catalytic performance that unprecedented with their parent metals because different components may have synergistic effects to obtain a new functional catalytic system.[225, 226]

Compared to single component noble metal nanocatalysts, the composite nanocatalysts possess several advantages. First, the incorporation of non-noble metals into noble metal based catalyst is helpful for cutting the cost, since the high price has become a major concern for all commercial technologies.[227] Many non-noble components, including Cu,[228, 229] Zn,[230, 231] and oxides[42, 232-235] generally act as promoters or supporters in composite catalysts, which can greatly decrease the content of noble metals. Additionally, the formation of composite nanomaterials can improve its stability by "diluting" the noble metal component. Second, composite catalysts can significantly enhance the catalytic performance due to the synergistic effects among different components. For example, the strong-metal-support-interaction (SMSI) between a metal catalyst and the support has proven to be very important for a lot of catalytic reactions. Third, the stability of composite nanomaterials can be improved by properly engineering its composition as well as architectures. For instance, a core-shell nanostructure that composed of a metallic core and a thermally stable shell shows much better thermal stability because the shell can separate the metal nanoparticles and prevent the agglomeration.[236] Fourth, composite nanoparticles may provide some additional functions by adding some specific components. For example, Xu and co-workers synthesized the Fe@Pt core-shell nanoparticles for ammonia borane oxidation. The composite catalyst could be magnetically recycled because of the magnetic properties of iron.[237] This kind of idea has been extended to some other systems, including Au-Co,[238] Au-Fe,[74] Ag-Fe,[239] Pd-Fe,[240, 241] Rh-Fe [242] and Pd-Co [243]. Further discussion on the catalytic performance of the composite nanoparticles is presented in Section 4.

4. Catalytic applications

As mentioned in the previous section, composite nanocatalysts show improved catalytic performance, including higher activity, longer lifetime, lower cost, and higher selectivity. Over the past several decades, various noble metal based composite nanocatalysts have been reported. In this Section, we will highlight some typical composite nanocatalysts, which can be roughly divided into three categories: bimetallic, tri-metallic and metal-oxide composites.

4.1 Bimetallic catalysts

Pt-Pd catalyst Pt-Pd composite catalysts have been widely studied for their potential application in oxygen reduction reaction (ORR), since Pt is the most effective catalyst to facilitate both hydrogen oxidation and oxygen reduction in a proton-exchange membrane (PEM) fuel cell.[244-246] Xia's group synthesized Pd-Pt bimetallic nanodendrites consisting of a dense array of Pt branches on a Pd core for the oxygen reduction reactions. The catalysts exhibited relatively large surface areas and particularly active facets toward the oxygen reduction reaction, showing 2.5 times higher activity on the basis of equivalent Pt mass than the state-of-the-art Pt/C catalyst and five times higher activity than the Pt-black catalyst (as shown in Figure 10).[244]

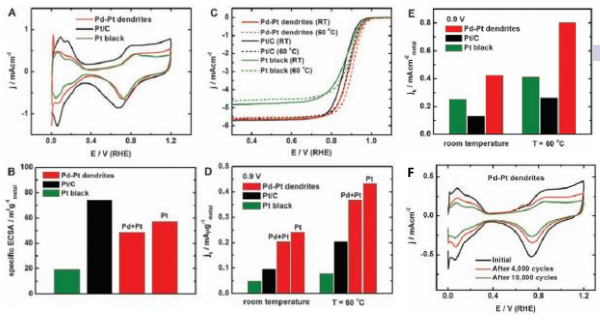

Figure 10. Comparison of electrocatalytic properties of the Pt-Pd nanodendrites, Pt/C catalyst (E-TEK) (20% by weight of 3.2-nm Pt nanoparticles on carbon support), and Pt black (Aldrich) (fuel cell grade). (A) CV curves recorded at room temperature in an Ar-purged 0.1M $HClO_4$ solution with a sweep rate of 50mV/s. (B) Specific ECSAs for the Pt-Pd nanodendrites, Pt/C catalyst, and Pt black. (C) ORR polarization curves for the Pd-Pt nanodendrites, Pt

catalyst, and Pt black recorded at room temperature and 60°C in an O_2-saturated 0.1 M $HClO_4$ solution with a sweep rate of 10 mV/s and a rotation rate of 1600 rpm. (D) Mass activity and (E) specific activity at 0.9 V versus RHE for these three catalysts. (F) CV curves for the Pt-Pd nanodendrites before and after accelerated durability test. Reproduced with permission from ref. 244. Copyright 2009 the American Association for the Advancement of Science.

Another account from Xia group describes Pt-Pd nanocages with hollow interiors and porous walls that exhibits both higher activity and selectivity for the preferential oxidation (PROX) of CO in excess hydrogen than those of Pd nanocubes and the commercial Pt/C (Figure 11 A-B).[121] The investigations on mechanism of Pt-Pd composite catalysts suggest that the catalytic performance of Pt-Pd composite nanoparticles strongly depends on their compositions and structures. For example, Hong *et al.*[247] have demonstrated that Pt-Pd nanocages with porous walls and dendritic hollow structures could enhance the catalytic performance of Pt-Pd catalyst in oxygen reduction reactions (Figure 11 C-D), while Yin *et al* have presented the enhanced electrocatalytic activity and durability of Pt-Pd tetrahedrons and cubes in ORR applications (Figure 11 E-F).[248]

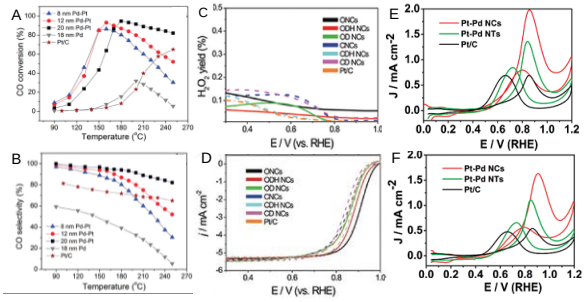

Figure 11. Plots of (A) activity and (B) selectivity as a function of reaction temperature for CO preferential oxidation in the presence of hydrogen on Pd-Pt alloy nanocages of 8, 12, and 20 nm in size, Pd nanocubes of 18 nm in size, and the commercial Pt/C catalyst. Reproduced with permission from ref.[121]. Copyright 2011 American Chemical Society. (C) H_2O_2 yield plots and (D) ORR polarization curves for the Pd-Pt bimetallic NCs and Pt/C obtained using a RRDE in O_2-saturated 0.1 M $HClO_4$ at scan rate of 10 mV s^{-1} and a rotation rate of 1600 rpm. Reproduced with permission from ref. 247. Copyright 2012 American Chemical Society. (E) Stable CV curves obtained for the Pt-Pd NCs, NTs, and Pt/C in the electrolyte of 0.1 M $HClO_4$ and 1 M CH_3OH at the sweep rate of 50 mV/s. (F) CV curves obtained after 4000 additional cycles. Reproduced with permission from ref. 248. Copyright 2011 American Chemical Society.

Pd-Ni The introduction of Ni element can significantly improve the catalytic performance of Pd catalysts. For example, Justus and co-workers have synthesized cavity-conform Ni-Pd nanoparticles for catalytic hydrogenation of dialkyl ketones. The catalytic performance of the composite Pd-Ni catalysts is highly dependent on the compositions, giving a much higher activity than the pure Pd or Ni catalysts (Figure 12).[249] Recently, the Kawai group has also shown that Pd-Ni bimetallic catalysts exhibited a higher activity than Pd towards the reduction of *p*-nitrophenol, even when the number of Pd atoms in Pd-Ni bimetallic nanowires was lower than pure Pd nanowires.[250] Son and co-workers have investigated the catalytic performance of Ni@Pd core-shell for Sonogashira coupling reactions.[83] Pd-Ni composite catalysts have also been used for the decomposition of methane to hydrogen and carbon nanofiber.[251]

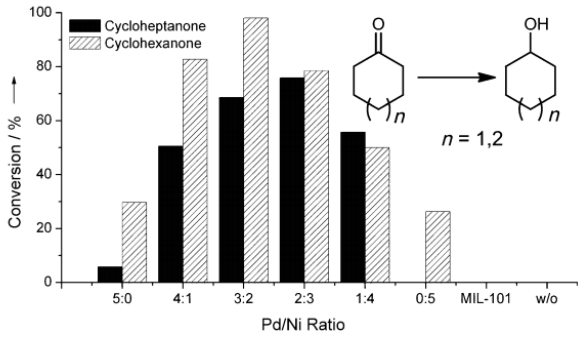

Figure 12. Reduction of cyclohexanone (0.18 mg Pd (0.52×10 mol %), 350 µL, 60 °C, 24 h) and cycloheptanone (0.36 mg P (0.8×10^{-3} mol %), 500 µL, 60 °C, 48 h) at 20 bar H_2; w/o = without catalyst. Reproduced with permission from ref. 249. Copyr 2012 Wiley-VCH Verlag GmbH & Co. KGaA, Weinheim.

Pd-Cu Pd-Cu bimetallic tripods with different compositions have been synthesized by a chemical reduction method and used for the catalytic oxidation of formic acid. The obtained Pd-Cu tripods hav highly accessible (211) facets on the side faces, which are expected to be an excellent catalyst for the electrocatalytic oxidation formic acid. Although only a minor difference between the catalytic activities of $Pd_{87}Cu_{13}$ and $Pd_{80}Cu_{20}$ was observed, the Pd-Cu tripod exhibited substantially enhanced (almost eight folds per unit mas of Pd) catalytic activity towards the electro-oxidation of formic acid comparing with the commercial Pd black (Figure 13).[228]

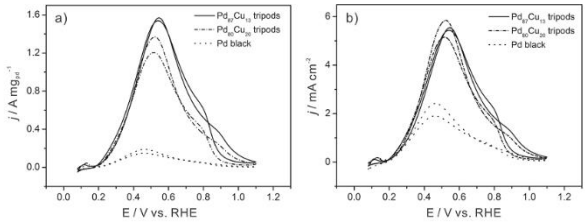

Figure 13. Cyclic voltammograms of the Pd-Cu tripods with different Pd to Cu ratios, together with that of commercial Pd blac The curve was recorded at room temperature in an aqueous solution containing 0.5 M HCOOH and 0.5 M $HClO_4$ at a sweeping rate of 50 mVs^{-1}. The current was normalized to the correspondir (a) mass of Pd and (b) ECSA, respectively. RHE: reversible hydrogen electrode. Reproduced with permission from ref. 228. Copyrigl 2014 Wiley-VCH Verlag GmbH & Co. KGaA, Weinheim.

A core-shell Cu@Pd core-shell catalyst for formic acid oxidatio was prepared by Li and co-workers by decorating Pd shell on th surface of Cu nanowire. Results from high-angle annular dark-fiel scanning transmission electron microscopy (HAADF-STEM) indicat that Cu only exists in the core part of the nanowire, while Pd mainly distributed in the shell part. The Cu@Pd core-shell nanoparticles exhibit good catalytic activity because of th synergetic effects of Cu and Pd (Figure 14).[252] Pd-Cu/Al_2O_3 catalysts have been prepared by Anderson and co-workers through impregnation method for selective acetylene hydrogenation.

optimized ratio of Cu and Pd in composite catalyst is about 50:1, giving a high acetylene conversion of 99 % and ethylene selectivity of 70 % at low temperature (100 °C). The enhanced activity is attributed to hydrogen dissociation on Pd with spill over to neighbouring Cu sites where the reaction takes place.[253] Gao and co-workers recently prepared montmorillonite (MMT)-supported Pd-Cu catalysts with narrow size distribution and well-controlled compositions for Sonogashira coupling reactions. The MMT@Pd/Cu material exhibit catalytic activity superior to MMT@Pd and MMT@Cu, giving a highest yield of products of 97 %.[254]

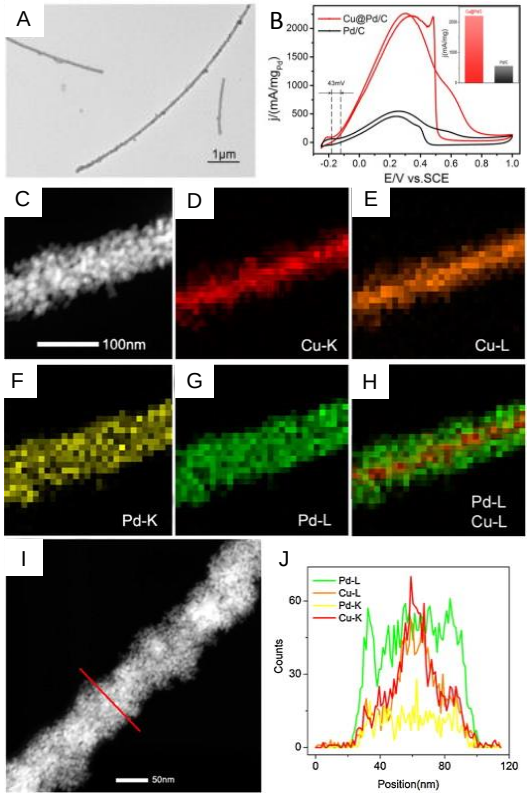

Figure 14. (A) TEM images of Cu@Pd nanowires. (B) Formic acid oxidation test of Cu@Pd/C and commercial Pd/C (N_2-saturated 0.1 M $HClO_4$+2 M HCOOH, Scan rate: 50 mV/s). The HAADF-STEM image of Cu@Pd nanowires (C), corresponding element mapping images of Cu-L (D), Cu-K (E), Pd-L (F), Pd-K (G), the 3d graphic illustration (H), and EDS line-scan analysis (I, J). Reproduced with permission from ref. 252. Copyright 2014 Elsevier Ltd.

Pd-Au Pd-Au composite nanoparticles have been studied for a number of different catalytic applications. Fortunellib and co-workers have investigated the CO oxidation process by using a combination of analytic-potential and first-principles density functional theory (DFT) calculations, suggesting that the composition of Pd-Au nanoparticles have a strong effects on the CO absorption and catalytic performance.[255] Hutchings *et al.* showed that Au/Pd-TiO_2 catalysts give very high turnover frequencies (up to 270,000 turnovers per hour) for the oxidation of alcohols, mainly because the addition of Au to Pd nanocrystals improved the overall selectivity (Figure 15 A-B).[42] The mechanism of the promotional effect of Au in a Pd-Au catalyst has been investigated by Goodman and co-workers. Results show that the role of Au is to isolate single Pd sites that facilitate the coupling of critical surface species to product, while inhibiting the formation of undesirable reaction by-products (Figure 15 C-D).[16]

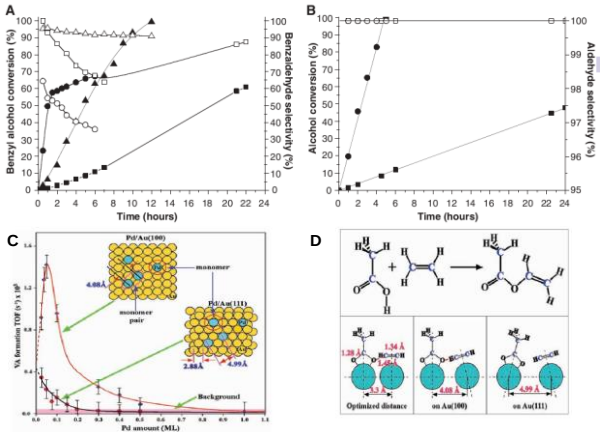

Figure 15. (A) Benzyl alcohol conversion and selectivity in benzaldehyde with the reaction time at 373 K and 0.1 MPa pO_2. Squares, Au/TiO_2; circles, Pd/TiO_2; and triangles, Au-Pd/TiO_2. Solid symbols indicate conversion, and open symbols indicate selectivity. (B) Au-Pd/TiO_2 catalyzed reactions at 363 K, 0.1 MPa pO_2, for cinnamyl alcohol (squares) and vanillyl alcohol (circles). Solid symbols indicate conversion, and open symbols indicate selectivity to the corresponding aldehydes. Reproduced with permission from ref.[42]. Copyright 2006 the American Association for the Advancement of Science. (C) Vinyl acetate (VA) formation rates (TOFs) as a function of Pd coverage on Au(100) and Au(111). The two insets show Pd monomers and monomer pairs on the Au(100) and Au(111) surfaces. (D) Schematic for VA synthesis from acetic acid and ethylene. The optimized distance between the two active centers for the coupling of surface ethylenic and acetate species to form VA is estimated to be 3.3 Å. With lateral displacement, coupling of an ethylenic and acetate species on a Pd monomer pair is possible on Au (100) but implausible on Au(111). Reproduced with permission from ref. 16. Copyright 2006 the American Association for the Advancement of Science.

Shim et al. investigated the electrocatalytic activity of spongelike nanoporous Pd-Au structures. The catalytic activity and stability of the Pd-Au catalyst are characterized for the oxygen reduction reactions in alkaline media. It is reported that the Pd-Au composite catalyst exhibited enhanced catalytic stability and comparable catalytic activity for the oxygen reduction reactions compared to the Pd-20/C and Pt-20/C products.[256] Pd-Au catalysts have also been used for selective hydrogen production *via* HCOOH decomposition by Mullins et al. It is found that the HCOOH molecules are activated by Pd atoms at the surface. Pd atoms that reside at Pd-Au interface sites favour the dehydrogenation of HCOOH, whereas at Pd(111)-like sites favour the dehydration of HCOOH, suggesting that the catalytic performance of Pd-Au catalysts on the decomposition of HCOOH can be tailored by controlling the arrangement of surface Pd and Au atoms.[257] Feng and co-workers have recently reported the catalytic oxidation of 1,2-propanediol with O_2 to lactic acid over hydroxylapatite nanorod-supported Au-Pd bimetallic nanoparticles (Au-Pd/HAP)

under atmospheric pressure. It is reported that the electron transfer between Au and Pd atoms can significantly enhance the catalyst performance, giving a maximum lactic acid selectivity of 97.1% and 1,2-propanediol conversion of 96.6%.[258]

Au-Pt Au-Pt composite nanoparticles have been used as efficient catalytic materials in fuel cell reactions. Suntivich and co-workers have established a direct correlation between the surface compositions of Au-Pt nanoparticles and their catalytic activities on CO and methanol oxidation. It is found that the intrinsic activities of Au-Pt nanoparticles with the same bulk composition of $Au_{0.5}Pt_{0.5}$ can be enhanced by orders of magnitude through simply controlling the surface composition. The phenomena can be attributed to the weakened CO binding on Pt in discrete Pt or Pt-rich clusters surrounded by surface Au atoms (Figure 16).[259]

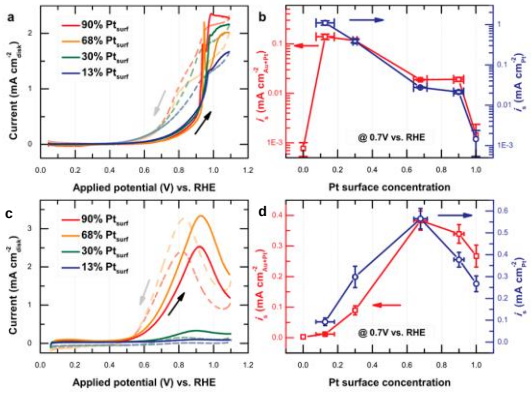

Figure 16. Activities of $Au_{0.5}Pt_{0.5}$ NPs at various surface compositions for carbon monoxide (a, b) and methanol electro-oxidation (c, d) reaction (COR). (a) As-measured COR current densities of $Au_{0.5}Pt_{0.5}$ NPs at various surface compositions in 0.1 M $HClO_4$. (b) The specific COR activities, i_s, $Au_{0.5}Pt_{0.5}$ nanoparticles (capacitance-corrected) normalized to either both Pt and Au surface area (red, left axis) or Pt surface area (blue, right axis) from a positive-going scan direction as a function of surface composition at 0.7 V vs RHE potential. (c) The methanol electro-oxidation reaction (MOR) geometric current densities of $Au_{0.5}Pt_{0.5}$ NPs at various surface compositions in 0.1 M $HClO_4$. (d) The specific MOR activities, i_s, of $Au_{0.5}Pt_{0.5}$ NPs (capacitance-corrected) normalized to either both Pt and Au surface area (red, left axis) or Pt surface area (blue, right axis) from the positive-going scan direction as a function of surface composition at 0.7 V vs RHE potential. The activity for 100% Pt was obtained from commercial Pt/C catalyst (Tanaka Kikinzoku). Reproduced with permission from ref. 259. Copyright 2013 American Chemical Society.

Wang *et al.* studied the mechanism of CO stripping on Pt@Au/C electrocatalysts with different Pt surface coverage by combining experimental analysis and density functional theory calculations. It is demonstrated that the formation of Pt-Pt surface of Pt atom and another neighbouring Pt atom is critical for CO adsorption and oxidation behaviours on the electrocatalyst.[260] Hyon and co-workers have reported Au@Pt core-shell nanoparticles for ethanol oxidation reactions, suggesting that the catalytic activity can be improved because the crystallinity of Pt shells can be promoted by the addition of Au.[261] Liu *et al.* have investigated the catalytic performance of carbon-supported Pt-Au nanorods with a core/shell structure on formic acid oxidation, showing that Pt species at the surface are critical for CO oxidation. Additionally, there is synergistic effect between Au and Pt species that can significantly enhance the catalytic performance in terms of activity and long term durability.[262] A similar result reported by Wang and co-workers indicates that the Au-Pt hybrid catalysts can effectively block CO formation and thus significantly increase the resistance to CO poisoning, giving a good stability towards oxygen reduction reactions with more than 2000 cycles.[263] X-ray absorption fine structure (XAFS) analysis suggests that the Pt-Pt bond distance and Au-Au bond distance of the Pt-Au/C catalyst is shorter than that of Pt foil and Au foil, and the shorter Pt-Pt bond distance as compared to that of Pt/C leads to the high oxygen reduction reactions activity of Pt/Au/C compared to that of Pt/C catalysts.[264] Another reason is that the synergistic effect between Au and Pt is favourable for increasing the concentration of surface-active oxygen (O_2^-) species which can enhance the catalytic performance of Au-Pt catalysts for oxidation.[265]

Ru-Pt Ru is another very important element for enhancing the catalytic performance of Pt based catalysts on a variety of fuel cell reactions.[266-268] In direct methanol fuel cells, Pt catalysts can be easily poisoned by CO, while Ru can help remove CO *via* preferential oxidation and thus improve the catalytic performance of Pt based catalysts. Hence, Ru-Pt composite nanoparticles have been widely used for the production of fuel cell electrodes. Manos and co-workers have investigated the Ru-Pt core-shell nanoparticles for preferential oxidation of carbon monoxide in hydrogen. It is found that Ru-Pt core-shell nanoparticles exhibits a much higher catalytic activity than traditional Pt-Ru composite, monometallic mixtures of nanoparticles or pure Pt particles (Figure 17).[47] Density functional theory studies suggest that the enhanced catalytic activity of the core-shell nanoparticle originates from a combination of an increased availability of CO-free Pt surface sites on the Ru@Pt nanoparticles and a hydrogen-mediated low-temperature CO oxidation process.[269] Oldfield et al have investigated the CO tolerance in a Pt/Ru fuel cell by using solid-state electrochemical (EC) NMR. Results show that the addition of Ru can weaken the metal-CO (d-π*) bond and lead to a lower activation barrier to CO thermal diffusion in the Pt/Ru domains.[270]

Besides, the catalytic performance of Ru-Pt composite catalysts strongly depended on the compositions and morphologies.[271, 272] For example, an account from Navaneethan and co-workers have studied the effects of structure on catalytic performance, showing that 10-fold higher for Ru-Pt alloy shells and 5-fold higher for Pt enriched shells comparing with the pure Pt catalyst.[271] Johansson *et al.* have synthesized the Pt-Ru catalysts with various compositions of Ru for the CO oxidation and methanol oxidation reaction. It is found that the activity is low for pure Pt and it is gradually reduced with increasing Ru content from 29 % up to 100 %.[272]

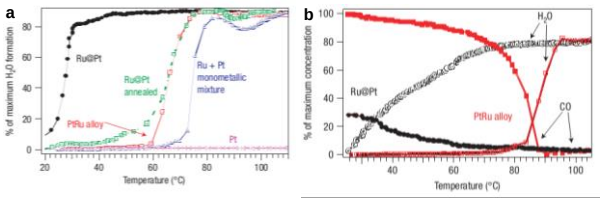

Figure 17. Catalytic results of core-shell and alloy Pt-Ru particles. (a) TPR results for the different Pt-Ru catalysts showing H_2O formation versus temperature for H_2 feeds contaminated by 0.1% CO by volume. The H_2O yields are plotted as % maximum formation based on the limiting reactant O_2. With complete CO conversion in the 0.1% CO feed, the maximum formation of water is 90%. The monometallic Pt remains in the baseline in this temperature range and does not light off until 170 ^{o}C. (b) % formation of H_2O (open symbols) and % CO conversion (filled symbols) plotted against temperature for the core-shell (black) and alloy (red) nanoparticles catalysts for H_2 feeds contaminated by 0.2% CO. In these feeds, the maximum H_2O yield is 80% when CO is preferentially oxidized. CO is normalized to its inlet concentration. Reproduced with permission from ref. [269]. Copyright 2008 Nature Publishing Group.

Au-Ni The Au-Ni composite catalyst shows much higher stability than monometallic Ni and Au catalysts. For example, Jiang and co-workers reported Au-Ni@SiO_2 composite catalysts with higher catalytic activity and better durability toward the hydrolysis of ammonia borane. It is found that Au-Ni@SiO_2 catalyst exhibits enhanced activity and stability in the generation of hydrogen, giving the greatest hydrogen productivity in the shortest time comparing with Au@SiO_2 catalyst and Ni@SiO_2 catalyst.[273] Besenbacher and co-workers studied low-temperature CO oxidation on Ni(111) and Au/Ni(111) surface. It is shown that low-temperature CO oxidation can be rationalized by CO oxidation on O_2-saturated NiO(111) surfaces. The main effect of Au on the Au/Ni(111) surface is to block the formation of carbonate and thereby increase the catalytic activity toward low-temperature CO_2 production.[274] Au-Ni nanoparticles supported on SiO_2 and TiO_2 have also been studied by Keane in catalytic hydrodechlorination. The TiO_2-supported Au-Ni catalysts exhibit much higher specific hydrodechlorination rates and distinct selectivity than the SiO_2 systems, suggesting that the supporter is one of the critical factors to obtain catalysts with excellent activity and stability.[275] The structure and reactivity of SiO_2 and $MgAl_2O_4$ supported Ni-Au nanoparticle catalysts have been reported by Alfons and Jens by using a combination of *in situ* X-ray absorption fine structure, transmission electron microscopy, and *in situ* X-ray powder diffraction. It is found that Au-Ni composite particles exhibit much higher activity and stability than pure Ni. The Au atoms appear to block the high reactivity edge and kink sites on the small Ni particles, and thus lower the probability of adsorbed carbon to form graphite and carbon whiskers.[276] Another important factor for enhancing the stability of Au-Ni catalysts is that the introduction of Au in Ni-based catalysts can retard carbon formation during reactions.[277, 278]

Other bimetallic catalysts Pt-Rh alloy nanoparticles have also been used in methanol electrooxidation reaction because of the improved electrocatalytic activity and stability. The composite Pt-Rh catalysts with well-defined alloy formation, uniform particle size and shape, and high-index facets exhibit improved electrocatalytic activity and stability in comparison with spherical Pt-Rh and pure Pt nanoparticles.[279] Farrauto and co-workers have investigated the catalytic performance of Rh-Pt catalyst on steam reforming of sulfur-containing dodecane, suggesting that higher steam/carbon ratio positively favours the stability of catalyst.[280] Rh-Sn/SiO_2 bimetallic catalysts have been prepared by Basset and co-workers for propane dehydrogenation. It is found that the inactive Sn on the surface of Pt nanoparticles can isolate the active Pt atoms, resulting in the enhanced catalytic performance on the dehydrogenation of propane.[281] Xiang and co-workers have studied the catalytic performance of various supported Pt-Sn catalysts for propane dehydrogenation, suggesting that supporters are quite important for enhancing catalytic activity and stability.[282] In addition, many reports show that mixing non-noble metals to replace or decrease the noble metal can not only increase the catalytic performance, but also decrease the cost of catalyst preparation. For example, Linic and co-workers have demonstrated low-cost Ag-Co surface alloy nanoparticle for oxygen reduction reaction, in which cheap metals have been used to replace conventional Pt-based catalysts. Comparing with the conventional Pt catalyst, the performance of Ag-Co bimetallic catalysts reaches over half of the area-specific activity of Pt catalysts and is more than a fivefold improvement over pure silver nanoparticles at typical operating potentials.[283] Weckhuysen *et al.* recently reported Pt-promoted Ga/Al_2O_3 catalyst for the dehydrogenation of propane.[284] The Pt-Ga/Al_2O_3 catalysts prepared by impregnation methods exhibit high activity, selectivity and stability on the dehydrogenation of propane, giving a maximum propane conversion of 42 % and propene selectivity of 96% even when the content of Pt is as low as 1000 ppm (Figure 18). The authors claim that Ga is the active species where Pt functions as a promoter. This is in striking contrast with the conventional Pt-Ga catalysts, in which Ga is regarded as a promoter and Pt is the active element.[285, 286] Other composite bimetallic catalysts, including Pd-Sn catalysts,[287, 288] Pd-Zn catalysts,[230, 289, 290], Pt-Ni catalysts,[291] Pt-Fe,[292] and Rh-Cu catalysts[293] have been reported for catalytic reactions, showing that the introduction of a second non-noble metals can significantly enhance the catalytic activity of monometallic catalysts.

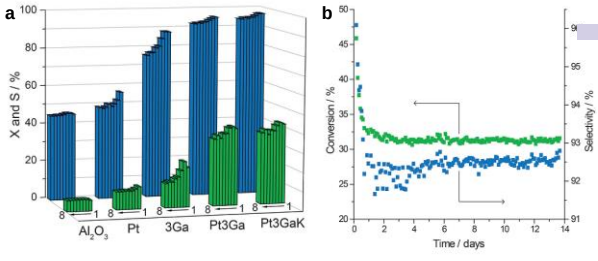

Figure 18. (a) Conversion of propane (X, green) and selectivity (S, blue) for propene during propane dehydrogenation on the Al_2O_3 support, Pt, 3Ga, Pt_3Ga, and Pt_3GaK catalysts for each of the eight successive dehydrogenation cycles. The exact values of X and S for the first, second, and eighth cycle. (b) Long-term stability experiment with the Pt_3GaK catalyst, which was cycled for ca. 15

times over a 14 day period. Reproduced with permission from ref. 284. Copyright 2014 Wiley-VCH Verlag GmbH & Co. KGaA, Weinheim.

Phase segregation of bimetallic nanoparticles An interesting study conducted by Somorjai and co-workers demonstrated that the composition of bimetallic nanoparticles can be varied by changing the reaction condition. They studied both $Rh_{0.5}Pd_{0.5}$ and $Pt_{0.5}Pd_{0.5}$ nanoparticles under oxidizing, reducing, and catalytic conditions by using x-ray photoelectron spectroscopy at near ambient pressure. Under oxidizing condition (100 mtorr NO or O_2), $Rh_{0.5}Pd_{0.5}$ nanoparticles has a Rh-rich shell with most of the Rh in the oxide form. Under both catalytic condition (100 mtorr NO and 100 mtorr CO) and reducing condition (100 mtorr CO or hydrogen), the shell become more Pd-rich (Figure 19)[191]. The composition change and oxidation states change are highly reversible. The reversible segregation phenomena in bimetallic nanoparticles have been ascribed to the surface energy in the metals and oxides. The surface energy of Pd is relatively lower than that of Rh, while Rh oxide is more stable than Pd oxide. As a result, Rh atoms tend to stay outside under oxidative condition and migrate into the core under reductive condition. As a comparison, no substantial segregation of Pd or Pt atoms was found in $Pt_{0.5}Pd_{0.5}$ nanoparticles.

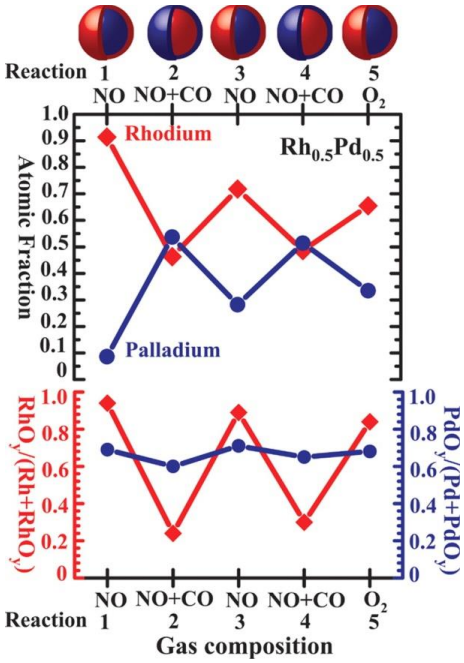

Figure 19. (Top) Evolution of Rh (Rh^0 + Rh^{2y+}) and Pd (Pd^0 + Pd^{2y+}) atomic fractions in the $Rh_{0.5}Pd_{0.5}$ NPs at 300°C under oxidizing conditions (100 mtorr NO or O_2) and catalytic conditions (100 mtorr NO and 100 mtorr CO) denoted in the x axis. (Bottom) Evolution of the fraction of the oxidized Rh (left y axis) and Pd atoms (right y axis) in the examined region under the same reaction conditions as the top part of the figure. All atomic fractions in this figure were obtained with an x-ray energy of 645 eV for Rh3d and Pd3d, which generates photoelectrons with a MFP of ~0.7 nm. Schematic diagrams above the top of the figure show the reversible segregation of Rh and Pd under alternating oxidizing and catalytic conditions. The y-axis data points for reactions 1, 3, and 5 have an associated error of ±0.03; for reactions 2 and 4, the error bar is ±0.02. Reproduced with permission from ref. 191. Copyright 2009 the American Association for the Advancement of Science.

4.2 Tri-metallic catalysts

Recently, the preparation of composite catalysts with more components has attracted some attention, because it is believed that such complicated system might show unprecedented catalytic performance. For example, Hungria and co-workers have reported the application of tri-metallic Ru_5PtSn nanoparticles in single-step conversion of dimethyl terephthalate (DMT) into cyclohexanedimethanol (CHDM). It is believed that Sn in the composite catalyst played a key role in anchoring the particle owing to its oxophilicity to the support, which in turn diminishes the tendency for the nanoparticles to sinter.[294] Pt_3Ni@Au tri-metallic catalysts have been synthesized by Li group for the Suzuki Miyaura reaction and reduction of nitrobenzene using formic acid. It is found that the catalytic performance can be significantly improved by sophisticated decoration with the third metal (Figure 20).[295]

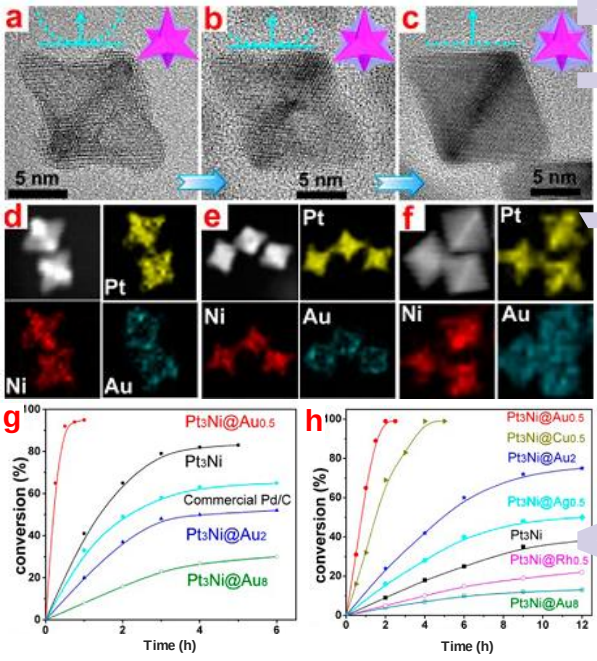

Figure 20. (a-c) SA-corrected HRTEM images of (a) $Pt_3Ni@Au_0$, (b) $Pt_3Ni@Au_2$, and (c) $Pt_3Ni@Au_8$. (d-f) Elemental mapping of (a) $Pt_3Ni@Au_{0.5}$, (e) $Pt_3Ni@Au_2$, and (f) $Pt_3Ni@Au_8$. Conversion as a function of time in the Suzuki-Miyaura reaction (g) and reduction of nitrobenzene using formic acid as a hydrogen source catalyzed by tri-metallic catalysts containing 0.5 atom %Pt (h). Reproduced with permission from ref.[295]. Copyright 2013 American Chemical Society.

Tri-metallic Au-Pd-Pt nanostructures are highly active and fairly stable when employed as anode catalysts for electro-oxidation. Wang and Yamauchi have synthesized tri-metallic Au@Pd@Pt core-shell nanoparticles as an efficient catalyst for methanol oxidation reaction. It is found that the pseudo inserted Pd-Pt alloy can serve as catalytic sites, while the Au cores serve as only the seed for subsequent deposition of the Pd inner layer and Pt outer shell.

Another account shows that very few Au atoms (the surface atomic ratio of Pt/Pd/Au is 15:102:1) on the surface of tri-metallic Au@Pd@Pt concave nanocubes lead to excellent catalytic performance on ethanol electro-oxidation due to the synergistic effects among the metals.[297]

Pt based tri-metallic nanoparticles have also been used for oxygen reduction reactions due to their high activity for fuel oxidation and oxygen reduction reactions.[298-300] Xia's group recently reported tri-metallic Pd@Pt-Ni core-shell octahedra catalysts for oxygen reduction reactions. It is found that the Pd@Pt-Ni/C catalyst shows an oxygen reduction reaction mass activity of 12.5-fold higher and a specific activity of 14-fold greater than that of the state-of-the-art Pt/C catalyst after HAc treatment.[301] The introduction of Ni into Pt based catalysts can effectively increase the specific activity because Ni can tune the d-band center and surface structure of Pt.[302, 303] Furthermore, the metal of Co can increase the activity of Pt-Pd towards the oxygen reduction reactions, giving enhanced mass activity, specific activity, durability and methanol tolerance in the oxygen reduction reaction compared with commercially available Pt black.[304, 305] Sun and co-workers recently reported Ag/CuPd and Au/CuPd tri-metallic nanoparticles for oxygen reduction reactions, giving a mass activity of about 0.20 A/mg and 77.6% of their activity after 48000 s *i-t* test, which are more efficient than the commercial Pt catalysts (Figure 21).[306]

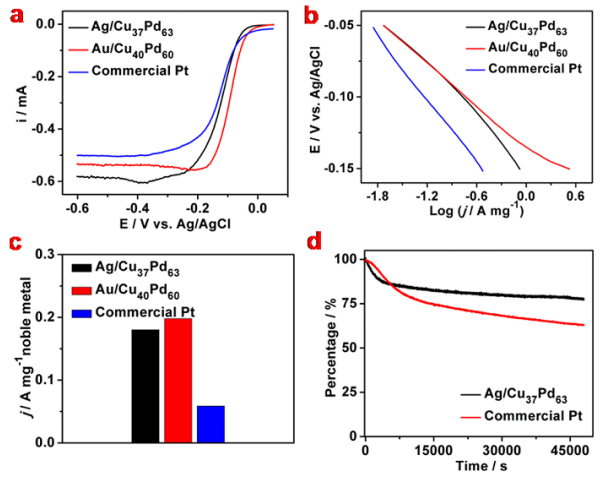

Figure 21. (a-c) Oxygen reduction reaction polarization curves (a), Tafel plots (b), and oxygen reduction reaction mass activity summaries (c) at -0.1 V of $Ag/Cu_{37}Pd_{63}$, $Au/Cu_{40}Pd_{60}$, and commercial Pt in O_2-saturated 0.1 M KOH solution at 293 K. Scan rate: 10 mV/s. Rotation rate: 400 rpm. (d) Chronoamperometric responses for the oxygen reduction reaction on $Ag/Cu_{37}Pd_{63}$ NPs and commercial Pt at -0.3 V. Rotation rate: 200 rpm. Reproduced with permission from ref. 306. Copyright 2014 American Chemical Society.

4.3 Metal-Oxide Composite Catalysts

Long before the rising of nanotechnology, people were able to make various metal-oxide composite catalysts. With the development of nanotechnology, we are able to make composite nanocatalysts with well defined shape, composition, and interface. As a result, we can understand the underneath mechanism, which in turn, help us design and make new catalysts. In this Section, we will highlight some metal-oxide composite system, including TiO_2, ZnO, Al_2O_3, SiO_2 and CeO_2.

Metal-TiO_2 TiO_2 is an important semiconductor with a relatively wide band-gap (~3.2 eV for anatase TiO_2), which usually can utilize only UV light. Recently, it is realized that one can make Au/Ag-TiO_2 hybrid nanostructure to extend the absorption to longer wavelength by utilizing the SPR property of Au or Ag. In addition, the metal component can help to separate the electron and hole and thus improve its catalytic property.

For example, Yang and co-workers have studied the catalytic performance of Au-TiO_2 for oxidizing CO under visible light irradiation.[307] It is found that the visible light can promote the preferential oxidation of CO over Au-TiO_2 catalyst comparing with Au-Al_2O_3 catalyst (Table 1). The irradiated light may result much more O_{act} species on TiO_2 surface, which is considered as the critical factor in photocatalysis of CO *via* a so-called Au-assisted Mars-van Krevelen mechanism.[308] Liang and co-workers have studied the oxidation of methanol to methyl formate on Au-Ag/TiO_2 catalyst under UV irradiation. It is found that Au-Ag/TiO_2 catalysts exhibit superior photocatalytic performance in terms of high methanol conversion of 90% and methyl formate selectivity of 85%.[309] Llorca and co-workers have reported hydrogen production from the photolysis of ethanol-water over Au/TiO_2 catalyst, the catalytic performance was strongly depended on catalyst loading, Au content, temperature, contact time and water to ethanol composition.[310] Gao and Yin recently synthesized Au/TiO_2 photocatalysts by depositing pre-synthesized colloidal Au nanoparticles with well-controlled sizes to TiO_2 nanocrystals and then removing capping ligands on the Au surface through a delicately designed ligand-exchange method. The obtained catalyst has a very clean surface, showing a superior activity in both dye decomposition and water-reduction hydrogen production (Figure 22).

Table 1 Catalytic performances for oxidizing CO in the absence or presence of H_2 over Au/TiO_2 and Au/Al_2O_3 at 20 °C under visible light irradiation or not, respectively.

Catalysts	Conversion of CO (%)		Conversion of H_2 (%)		Selectivity of CO oxidation (%)	
	No light[b]	Light[c]	No light	Light	No light	Light
Au-TiO_2[d]	64.1	79.6	-	-	-	-
Au-Al_2O_3[d]	23.6	25.2	-	-	-	-
Au-TiO_2[e]	30.3	37.1	8.6	7.9	66.7	68.0
Au-Al_2O_3[e]	23.5	25.1	1.3	1.6	92.6	88.5

a: Selectivity of CO oxidation is defined as the ratio of O_2 consumption for oxidizing CO to the total O_2 consumption; ***b***: No light: Reaction under dark; ***c***: Light: Reaction under visible light irradiation; ***d***: Oxidizing CO in the absence of H_2; ***e***: Oxidizing CO in the presence of H_2. Reproduced with permission from ref.307. Copyright 2014 Elsevier Inc.

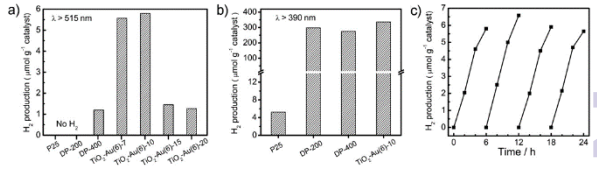

Figure 22. Photocatalytic hydrogen generation from the TiO_2-Au(*x*)-*y* nanocomposites under visible-light illumination in a period of 6 h. Bare P25 and Au/TiO_2 nanocomposites obtained by the DP method (DP-*x*; *x*, annealing temperature, °C; Au loading, 6 wt %) were employed as the control materials. (a) Illumination conditions: λ > 515 nm, 100 mW cm^{-2}. (b) Illumination conditions: λ > 390 nm, 100 mW cm^{-2} . (c) Photocatalytic hydrogen production from the photocatalyst TiO_2-Au(6)-10 in 4 cycles; illumination conditions: λ > 515 nm; 100 mW cm^{-2}. Reproduced with permission from ref.[311]. Copyright 2014 American Chemical Society.

Yin and co-workers have designed and fabricated a sandwich-like structured composite, in which Au nanoparticles are sandwiched by a silica core and a titania shell (as shown in Figure 23).[161] The addition of suitable amount of Au nanoparticles can significantly improve the photocatalytic performance of TiO_2. It is demonstrated that the sandwich structure shows much better performance in the photodegradation of organic dyes under direct sunshine than commercial P25 even when the loading of Au is only 5000 ppm.

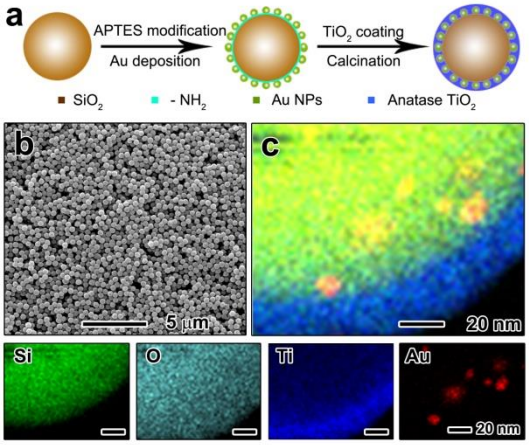

Figure 23. (a) Schematic illustration of the fabrication process of SiO_2@Au@TiO_2 sandwich-structured composite catalyst; (b) Typical SEM image of the composite catalyst. (c) Elemental mapping of a single particle, with the distribution of individual elements shown in the bottom row. Adapted with permission from Ref. 161. Copyright 2011 Wiley-VCH Verlag GmbH & Co. KGaA, Weinheim.

Additionally, metal-TiO_2 catalysts demonstrate exceptional catalytic activity for a wide range of reactions, such as CO oxidation, olefin epoxidation, hydrocarbons decomposition, and water gas shift (WGS) reaction.[312-319] For example, Li and Zeng have studied the reaction of CO with lattice oxygen atoms at the Au_{16}-TiO_2 interface by using Born-Oppenheimer molecular dynamics (BOMD) simulation, suggesting that the M-vK mechanism is likely more favoured for relatively fluxional Au clusters, whereas the L-H mechanism is more favored for robust Au clusters.[320] Boughton and co-workers have reported a well-dispersed small Au-Ag composite catalyst on TiO_2 nanobelts that exhibited unique properties including high thermal stability, large surface area, high permeability, low density, and tailorable shape and size, giving an enhanced catalytic performance toward aerobic oxidation of benzyl alcohol.[321] Alberto and co-workers have prepared Au-Ag/TiO_2 catalysts by using deposition-precipitation method for the oxidation of CO. It is found that the Au-Ag/TiO_2 catalysts exhibit significantly higher activity and stability in CO oxidation, which can bear a high temperature of 550 °C.[322]

Metal-ZnO ZnO is also an important semiconductor. Metal-ZnO composites have been widely used in catalysis. Ravishankar and co-workers synthesized Au-ZnO nanohybrids by rapid microwave-assisted synthesis for CO oxidation. It is found that the presence of Au-Zn and Au-O bonds on the interface leads to the formation of anionic and cationic Au sites, which can significantly enhance the activity of the Au-ZnO catalysts.[323] Wanchanthuek and co-workers have prepared Au-ZnO catalysts through photodeposition method for CO oxidation. It is found that the small nanoparticles with a size of 1-2 nm can efficiently catalyze the preferential oxidation of CO.[324] An account from Wang has investigated the adsorption of CO on Au-ZnO catalyst through Fourier transform infrared (FTIR) spectroscopy in an ultra-high-vacuum (UHV) system. The proposed mechanism claims that O_2 absorbs on the Au/ZnO interface and reacts with the adsorbed CO to form the OC–O_2 intermediate complex, accompanied by charge transfer from substrate to O_2. Different carbonate species are produced via interaction of formed CO_2 with surface oxygen atoms on ZnO.[325] The first-principle investigations of Au catalysis on 2D one-atom-thick ZnO nanosheets on CO oxidation indicate that the planar structure (P2) of Au_3 cluster on 2d ZnO sheets exhibits high catalytic performance with a low reaction barrier of around 0.3 eV.[326]

Metal-ZnO nanoparticles have also been used as photocatalyst. For instance, Singla and co-workers have studied the photocatalytic activity of Au@ZnO core-shell nanostructure by the degradation of methyl orange (MO) dye and oxidation of methanol under visible irradiation, showing that the photocatalytic activity increased by the plasmonic Au core.[327] A similar enhancement has been reported by Wang and co-workers who have investigated the plasmonic heating effect of Au-ZnO on CO_2 reduction under visible light illumination. It is found that the conversion of CO_2 and the selectivity of products can be readily controlled by adjusting the light intensity (Fig. 24).[328]

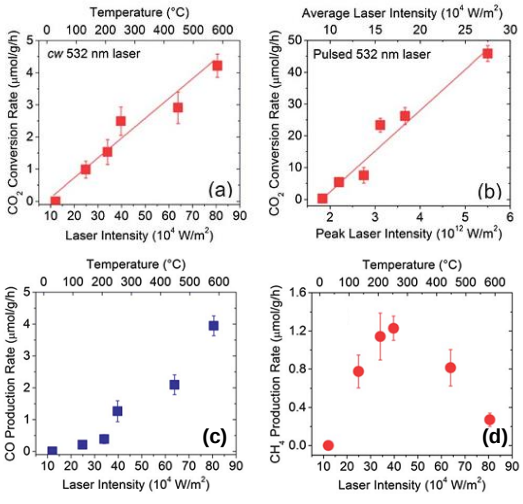

Figure 24. Catalytic CO_2 conversion rate as a function of laser intensity of (a) Au-ZnO under cw 532 nm illumination, with the corresponding catalyst temperature due to plasmonic heating

determined from Raman spectroscopic measurement as the top x-axis; and (b) Au-ZnO under pulsed 532 nm laser excitation. (c) CO production rate and (d) CH_4 production rate as a function of cw 532 nm laser intensity using Au-ZnO catalysts. Reproduced with permission from ref. 328. Copyright 2013 Royal Society of Chemistry.

Ag-Al_2O_3 Ethylene epoxidation is a process in which ethylene and oxygen react to form ethylene oxide (EO), which provides a gateway to produce ethylene glycol, ethanolamines, detergents, and many other chemicals in chemical industrials. Silver is the only heterogeneous catalyst that can achieve reasonable selectivity to EO. Linic's group has studied the ethylene epoxidation reaction by using Ag catalysts and suggested that heterogeneous composite Ag catalysts are more selective in partial oxidation of ethylene to form EO than conventional Ag catalysts.[329] Another account from the Linic group reported that the plasmonic silver nanosturcutres can concurrently use low-intensity visible light (on the order of solar intensity) and thermal energy to drive the ethylene epoxidation reaction.[330, 331] The so-called visible-light-enhanced catalytic process is quite important for ethylene epoxidation reaction to improve the catalytic performance by combing the thermal energy and laser irradiation. Conventional catalysts are driven by thermal energy, but high temperature may decrease the selectivity for the desired products because they are easily thermally activated on the catalyst. On the other hand, high operating temperature is another challenge for the stability of catalyst which may decrease or even lose the activity through carbon deposition and sintering.[332, 333] Mechanistic studies show that the plasmonic Ag nanocubes supported on Al_2O_3 (Ag-Al_2O_3) can yield chemically useful energetic electrons when irradiated with visible light, and these electrons can synergistically drive the ethylene epoxidation reaction with thermal energy (shown in Figure 25).

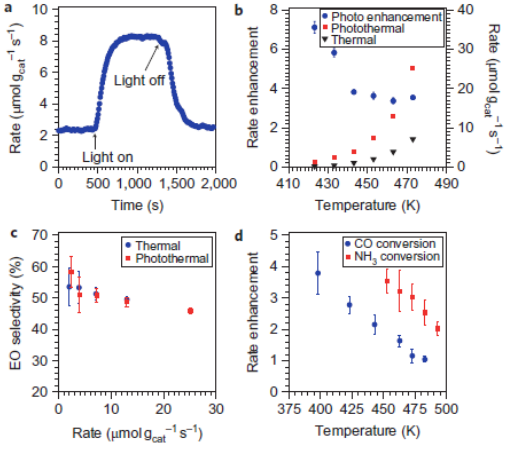

Figure 25. Plasmon-enhanced oxidation reactions. **a**, The rate of ethylene epoxidation at 450 K in the dark and with visible illumination. A significant enhancement in the rate caused by visible-light illumination was observed. **b**, Rate enhancement (left axis, blue circles) calculated by dividing the rate of the photothermal process by the rate of the thermal process as a function of temperature. On the right axis black triangles show the rate of thermal ethylene epoxidation and red squares show the rate of photothermal epoxidation as a function of temperature. **c**, Selectivity to EO for the thermal and photothermal processes as a function of reaction rate. The two processes show identical selectivity at a given rate. **d**, Rate enhancements, calculated by dividing the rate of photothermal by the rate of the pure thermal process, for CO and NH_3 oxidation as a function of temperature. Error bars in the plots represent the standard deviation of the systematic errors in the collection of mass spectrometer data. Reproduced with permission from ref. 330. Copyright 2011 Macmillan Publishers Limited.

Pt-SiO_2 Porous SiO_2 is a common supporter for synthesizing composite catalysts. A great number of mesopores in the SiO_2 can provide spaces for confining metal nanoparticles with specific size. The strong confinement effects of mesoporous SiO_2 can prevent the sintering of nanoparticles even under harsh conditions. The Pt-SiO_2 catalysts have been widely used in the past decades on hydrogenation reactions.[334, 335] Recently, Somorjai and co-workers studied the catalytic processes on Pt-SiO_2 catalysts during 1,3-butadiene hydrogenation by using *in situ* sum frequency generation vibrational spectroscopy (SFGVS), suggesting that calcination is effective in removing the capping agent PVP, and the SFGVS signal can be generated from the metal surface to monitor the catalytic processes.[336] Zhang's group reported a facile and scalable process to prepare graphene-nanosheet-supported Pt nanoparticles covered by mesoporous SiO_2 layers. The SiO_2 outer layer can restrain the π-π stacking interactions among graphene nanosheets supports and prevent the aggregation and restacking of graphene nanosheets. In addition, the confinement effects of mesoporous SiO_2 can prevent the sintering of Pt nanoparticles. These robust catalysts show high catalytic activity, high stability under high temperature calcination, and excellent recycling and reusability towards gas-phase and solution-phase reactions. [337]

Au-CeO_2 CeO_2 is one of the most efficient supporters for low-temperature oxidation of molecular CO due to its oxygen storage capacity. Camellone and Fabris have investigated the mechanism of CO oxidation on Au/CeO_2 catalysts, suggesting that the single gold atoms could promote the oxidation of CO on CeO_2 (111) surface. The reversible Au^{3+}/Au^{+} and Ce^{4+}/Ce^{3+} reductions assist the formation of surface O vacancies, and molecular oxygen can seal these vacancies to form activated O_{ad} species, leading to a local rearrangement of the AuO_4 unit activated by an energy barrier of 0.55 eV. CO reacts with these O_{ad} species without activation energy to form CO_2 and recover the initial stoichiometry of the $Au_xCe_{1-x}O$ system.[338] Another similar account for the CO oxidation mechanism on CeO_2-supported Au nanoparticles by using density functional theory (DFT) has been reported by Henkelman et al. They have compared CO oxidation by a Au_{13} nanoparticles supported on CeO_2 (Au_{13}@CeO2-STO) and partially reduced CeO_2 with three vacancies (Au_{13}@CeO_2-3VAC), giving three possible mechanisms as follows: (1) activating the M-*v*K mechanism of CO oxidation by lowering the energy of CO_2 production, (2) increasing the number of oxygen vacancies in the CeO_2 surface that bind and supply O_2 for the second half of the M-*v*K mechanism, and (3) increasing the concentration of reduced metal ions, which act as anchoring sites for O_2 molecules.[339]

5 Conclusion and Outlook

In this Review article, we have discussed the recent advances in noble metal based composite nanocatalysts. Incorporating another or many other components into a noble metal nanoparticle to form a composite can significantly improve its catalytic performance, such as activity, selectivity, and stability. We have mainly focused on the colloidal synthesis of bimetallic nanoparticles. With the development of nanotechnology, composite nanoparticles with desired shape, size, and physiochemical properties can be obtained through various approaches. We then highlighted some unique properties, especially SPR properties and magnetic properties, that are beneficial for the catalytic performance of nanomaterials. To the end, we have summarized some important catalytic applications of bimetallic, tri-metallic, and metal-oxide composite nanocatalysts.

One of the remaining challenges in this field is the characterization of nanocatalysts in the real reaction conditions. Although impressive progress has been achieved in understanding model reaction systems under some extreme condition, such as ultra-low pressure and low temperature, it is still very difficult to understand the phenomena under real reaction conditions, *e.g.*, high temperature and high pressure, due to the limitation of characterization tool. For example, although a lot of enhanced properties of composite catalysts have been ascribed to the synergistic effect, it is not clear where the synergistic effect come from and how we can design a structure that will have the effect. To reveal the synergistic effects of various elements, some *in situ* spectroscopic investigations and advanced characterizations are required to directly "see" the catalytic process. One of the potential techniques might be that based on synchrotron radiation. Since the aqueous phase reactions are more complicated, gas-phase reactions may be more easily to handle.

Another challenge is how to cut the cost of noble metal based catalysts to fulfil the requirement of industrial applications. To decrease the cost, one needs to decrease the content of noble metal. Recently, main-group and non-noble metal catalysis has attracted more and more attention. However, noble metals are still necessary for a lot of applications. A possible solution to this question might be the advanced nanotechnology that can not only understand the reaction phenomena, but also can make better composite catalysts. For example, it is not easy to control the bonding property of composite nanoparticles from the atomic scale. If one could achieve the atom-to-atom fabrication of catalyst, we may be able to make excellent catalyst with low cost in a more sustainable way.

In terms of the stability of shape- and composition-controlled nanocatalysts, more researches should be conducted. Although a lot of composite catalysts with significantly enhanced catalytic performance have been reported by controlling their morphology and composition, the long-term stability is still a big concern. Recently, coating the active and unstable nanoparticle with a porous and stable shell to form a core-shell nanostructure has proven to be an effective way for some specific catalyst systems. But most synthetic strategies are tedious and time-consuming. More researches need to be done along this direction.

In a short summary, noble metal based catalysts have attracted increasing attention due to their excellent catalytic performance. We have tried to present an up-to-date overview of this field, however, it is impossible to take into account all contributions to the field. We hope that this critical review can inspire researchers pursuing in the area of catalysis and nanotechnology to design the noble metal based composite catalysts with excellent activity, low cost, and stability.

Acknowledgements

We thank the funding support from the National Natural Science Foundation of China (21401135) and the Natural Science Foundation of Jiangsu Province (BK20140304). Y.X. thanks the Collaborative Innovation Center of Suzhou Nano Science and Technology (Nano-CIC) for the fellowship of "Collaborative Academic Training Program for Post-doctoral Fellows" and the postdoctoral starting funding support from Soochow University.

Notes and references

1 K. Zhou and Y. Li, *Angew. Chem. Int. Edit.*, 2012, **51**, 602-613.
2 P. K. Jain, X. Huang, I. H. El-Sayed and M. A. El-Sayed, *Accounts Chem. Res.*, 2008, **41**, 1578-1586.
3 E. C. Dreaden, A. M. Alkilany, X. Huang, C. J. Murphy and M. A. El-Sayed, *Chem. Soc. Rev.*, 2012, **41**, 2740-2779.
4 C. M. Cobley, J. Chen, E. C. Cho, L. V. Wang and Y. Xia, *Chem. Soc. Rev.*, 2011, **40**, 44-56.
5 M. E. Stewart, C. R. Anderton, L. B. Thompson, J. Maria, S. K. Gray,J. A. Rogers and R. G. Nuzzo, *Chem. Rev.*, 2008, 108, 494-521.
6 S. Eustis and M. A. El-Sayed, *Chem. Soc. Rev.*, 2006, **35**, 209-217.
7 K. Kneipp, H. Kneipp and J. Kneipp, *Accounts Chem. Res.*, 2006, **39**, 443-450.
8 C. J. Murphy, A. M. Gole, J. W. Stone, P. N. Sisco, A. M. Alkilany,E.C. Goldsmith and S. C. Baxter, *Accounts Chem. Res.*, 2008, **41**,1721-1730.
9 E. Boisselier and D. Astruc, *Chem. Soc. Rev.*, 2009, **38**, 1759-1782.
10 M. C. Daniel and D. Astruc, *Chem. Rev.*, 2004, **104**, 293-346.
11 A. S. K. Hashmi and G. J. Hutchings, *Angew. Chem. Int. Edit.*, 2006, **45**, 7896-7936.
12 D. J. Gorin and F. D. Toste, *Nature*, 2007, **446**, 395-403.
13 A. Corma and H. Garcia, *Chem. Soc. Rev.*, 2008, 37, 2096-2126.
14 M. D. Hughes, Y. J. Xu, P. Jenkins, P. McMorn, P. Landon, D. I. Enache, A. F. Carley, G. A. Attard, G. J. Hutchings, F. King, E. H. Stitt, P. Johnston, K. Griffin and C. J. Kiely, *Nature*, 2005, **437**, 1132-1135.
15 A. S. K. Hashmi and M. Rudolph, *Chem. Soc. Rev.*, 2008, **37**, 1766-1775.
16 M. S. Chen, D. Kumar, C. W. Yi and D. W. Goodman, *Science*, 2005, **310**, 291-293.

17 H. P. Liang, H. M. Zhang, J. S. Hu, Y. G. Guo, L. J. Wan and C. L. Bai, *Angew. Chem. Int. Edit.*, 2004, **43**, 1540-1543.
18 S. Pedireddy, H. K. Lee, W. W. Tjiu, I. Y. Phang, H. R. Tan, S. Q. Chua, C. Troadec and X. Y. Ling, *Nat. Commun.*, 2014, DOI: 10.1038/ncomms5947.
19 C. B. Gao, J. Vuong, Q. Zhang, Y. D. Liu and Y. D. Yin, *Nanoscale*, 2012, **4**, 2875-2878.
20 X. C. Ye, L. H. Jin, H. Caglayan, J. Chen, G. Z. Xing, C. Zheng, V. Doan-Nguyen, Y. J. Kang, N. Engheta, C. R. Kagan and C. B. Murray, *Acs Nano*, 2012, **6**, 2804-2817.
21 J. Wang, C.-K. Tsung, R. C. Hayward, Y. Wu and G. D. Stucky, *Angew. Chem. Int. Edit.*, 2004, **44**, 332-336.
22 Z. Y. Tang, N. A. Kotov and M. Giersig, *Science*, 2002, **297**, 237-240.
23 Y. Xu, X. Wang, L. Chen, Y. Zhao, L. He, P. Yang, H. Wu, F. Bao and Q. Zhang, *J. Mater. Chem. C*, 2015, **3**, 1447-1451.
24 Y. Xu, Y. Zhao, L. Chen, X. Wang, J. Sun, H. Wu, F. Bao, J. Fan and Q. Zhang, *Nanoscale*, 2015, **7**, 6790-6797.
25 L. Chen, F. Ji, Y. Xu, L. He, Y. Mi, F. Bao, B. Sun, X. Zhang and Q. Zhang, *Nano Lett.*, 2014, **14**, 7201-7206.
26 Y. Huang, A. R. Ferhan, Y. Gao, A. Dandapat and D.-H. Kim, *Nanoscale*, 2014, **6**, 6496-6500.
27 Y. G. Sun and Y. N. Xia, *Adv. Mater.*, 2003, **15**, 695-699.
28 Q. Zhang, N. Li, J. Goebl, Z. Lu and Y. Yin, *J. Am. Chem. Soc.*, 2011, **133**, 18931-18939.
29 Y. G. Sun, B. Mayers and Y. N. Xia, *Nano Lett.*, 2003, **3**, 675-679.
30 M. L. Personick, M. R. Langille, J. Zhang, N. Harris, G. C. Schatz and C. A. Mirkin, *J. Am. Chem. Soc.*, 2011, **133**, 6170-6173.
31 J. Zhang, M. R. Langille and C. A. Mirkin, *J. Am. Chem.l Soc.*, 2010, **132**, 12502-12510.
32 E. Roduner, *Chem. Soc. Rev.*, 2006, **35**, 583-592.
33 A. Cao, R. Lu and G. Veser, *Phys. Chem. Chem. Phys.*, 2010, **12**, 13499-13510.
34 L. De Rogatis, M. Cargnello, V. Gombac, B. Lorenzut, T. Montini and P. Fornasiero, *ChemSusChem*, 2010, **3**, 24-42.
35 G. A. Tsigdinos, *J. Am. Chem. Soc.*, 1984, **106**, 2490-2490.
36 D. M. Alonso, S. G. Wettstein and J. A. Dumesic, *Chem. Soc. Rev.*, 2012, **41**, 8075-8098.
37 M. Sankar, N. Dimitratos, P. J. Miedziak, P. P. Wells, C. J. Kiely and G. J. Hutchings, *Chem. Soc. Rev.*, 2012, **41**, 8099-8139.
38 T. Hundertmark, A. F. Littke, S. L. Buchwald and G. C. Fu, *Org. Lett.*, 2000, **2**, 1729-1731.
39 T. Hayashi, K. Tanaka and M. Haruta, *J. Catal.*, 1998, **178**, 566-575.
40 H. H. Kung, M. C. Kung and C. K. Costello, *J. Catal.*, 2003, **216**, 425-432.
41 E. D. Park and J. S. Lee, *J. Catal.*, 1999, **186**, 1-11.
42 D. I. Enache, J. K. Edwards, P. Landon, B. Solsona-Espriu, A. F. Carley, A. A. Herzing, M. Watanabe, C. J. Kiely, D. W. Knight and G. J. Hutchings, *Science*, 2006, **311**, 362-365.
43 Q. Fu, H. Saltsburg and M. Flytzani-Stephanopoulos, *Science*, 2003, **301**, 935-938.
44 Y. Liu, Z. Fang, L. Kuai and B. Geng, *Nanoscale*, 2014, **6**, 9791-9797.
45 Q. Tan, C. Du, G. Yin, P. Zuo, X. Cheng and M. Chen, *J. Catal.*, 2012, **295**, 217-222.
46. J. Ge, Q. Zhang, T. Zhang and Y. Yin, *Angew. Chem. Int. Edit.*, 2008, **47**, 8924-8928.
47 M. Ye, Q. Zhang, Y. Hu, J. Ge, Z. Lu, L. He, Z. Chen and Y. Yin, *Chem-Eur. J.*, 2010, **16**, 6243-6250.
48 F. Studt, F. Abild-Pedersen, T. Bligaard, R. Z. Sorensen, C. H. Christensen and J. K. Norskov, *Science*, 2008, **320**, 1320-1322.
49 F. Besenbacher, I. Chorkendorff, B. S. Clausen, B. Hammer, A. M. Molenbroek, J. K. Norskov and I. Stensgaard, *Science*, 1998, **279**, 1913-1915.
50 J. Greeley and M. Mavrikakis, *Nat. Mater.*, 2004, **3**, 810-815.
51 S. Garcia, L. Zhang, G. W. Piburn, G. Henkelman and S. M. Humphrey, *ACS Nano*, 2014, **8**, 11512-11521.
52 Q. Zhang, I. Lee, J. B. Joo, F. Zaera and Y. D. Yin, *Accounts Chem. Res.*, 2013, **46**, 1816-1824.
53 R. Ferrando, J. Jellinek and R. L. Johnston, *Chem. Rev.*, 2008, **108**, 845-910.
54 C. N. R. Rao, G. U. Kulkarni, P. J. Thomas and P. P. Edwards, *Chem. Soc. Rev.*, 2000, **29**, 27-35.
55 Y. Xiong, I. Washio, J. Chen, H. Cai, Z.-Y. Li and Y. Xia, *Langmuir*, 2006, **22**, 8563-8570.
56 X. Huang, S. Tang, X. Mu, Y. Dai, G. Chen, Z. Zhou, F. Ruan, Z. Yang and N. Zheng, *Nat. Nano*, 2011, 6, 28-32.
57 H. Li, G. Chen, H. Yang, X. Wang, J. Liang, P. Liu, M. Chen and N. Zheng, *Angew. Chem. Int. Edit.*, 2013, **52**, 8368-8372.
58 J. Chen, P. Xiao, J. Gu, D. Han, J. Zhang, A. Sun, W. Wang and T. Chen, *Chem. Commun.*, 2014, **50**, 1212-1214.
59 K. A. Kuttiyiel, K. Sasaki, Y. Choi, D. Su, P. Liu and R. R. Adzic, *Nano Lett.*, 2012, **12**, 6266-6271.
60 R. Su, R. Tiruvalam, Q. He, N. Dimitratos, L. Kesavan, C. Hammond, J. A. Lopez-Sanchez, R. Bechstein, C. J. Kiely, G. J. Hutchings and F. Besenbacher, *Acs Nano*, 2012, **6**, 6284-6292.
61 F. Wen, W. Zhang, G. Wei, Y. Wang, J. Zhang, M. Zhang and L. Shi, *Chem. Mater.*, 2008, **20**, 2144-2150.
62 H. Yang, Y. Wang, J. Lei, L. Shi, X. Wu, V. Maekinen, S. Lin, Z. Tang, J. He, H. Haekkinen, L. Zheng and N. Zheng, *J. Am. Chem. Soc.*, 2013, **135**, 9568-9571.
63 S. Shen, J. Zhuang, Y. Yang and X. Wang, *Nanoscale*, 2011, **3**, 272-279.
64 C. Li, Z. Shao, M. Pang, C. T. Williams, X. Zhang and C. Liang, *Ind. Eng. Chem. Res.*, 2012, **51**, 4934-4941.
65 S. Guo, L. Wang, S. Dong and E. Wang, *J. Phys. Chem. C*, 2008, **112**, 13510-13515.
66 I. Lee, J. B. Joo, Y. Yin and F. Zaera, *Angew. Chem. Int. Edit.*, 2011, **50**, 10208-10211.
67 L. A. Pretzer, H. J. Song, Y.-L. Fang, Z. Zhao, N. Guo, T. Wu, I. Arslan, J. T. Miller and M. S. Wong, *J. Catal.*, 2013, **298**, 206-217.
68 J. Li and H. C. Zeng, *Angew. Chem. Int. Edit.*, 2005, **44**, 4342-4345.
69 S. Wu, J. Dzubiella, J. Kaiser, M. Drechsler, X. Guo, M. Ballauff and Y. Lu, *Angew. Chem. Int. Edit.*, 2012, **51**, 2229-2233.
70 V. Mazumder, M. Chi, K. L. More and S. Sun, *Angew. Chem. Int. Edit.*, 2010, **49**, 9368-9372.
71 S. Sun, G. Zhang, D. Geng, Y. Chen, R. Li, M. Cai and X. Sun, *Angew. Chem. Int. Edit.*, 2011, **50**, 422-426.
72 H.-S. Shin and S. Huh, *ACS Appl. Mater. Inter.*, 2012, **4**, 6324-6331.

73 K. M. Manesh, A. I. Gopalan, K.-P. Lee and S. Komathi, *Catal. Commun.*, 2010, **11**, 913-918.
74 F.-H. Lin and R.-A. Doong, *J. Phys. Chem. C*, 2011, **115**, 6591-6598.
75 F. Taufany, C.-J. Pan, H.-L. Chou, J. Rick, Y.-S. Chen, D.-G. Liu, J.-F. Lee, M.-T. Tang and B.-J. Hwang, *Chem-Eur. J.*, 2011, **17**, 10724-10735.
76 D. Wang and Y. Li, *J. Am. Chem. Soc.*, 2010, **132**, 6280-6281.
77 D. Wang, Q. Peng and Y. Li, *Nano Res.*, 2010, **3**, 574-580.
78 T. Ward, L. Delannoy, R. Hahn, S. Kendell, C. J. Pursell, C. Louis and B. D. Chandler, *ACS Catal.*, 2013, **3**, 2644-2653.
79 X. Yang, D. Chen, S. Liao, H. Song, Y. Li, Z. Fu and Y. Su, *J. Catal.*, 2012, **291**, 36-43.
80 S. Xia, Z. Yuan, L. Wang, P. Chen and Z. Hou, *Appl. Catal. A-Gen.*, 2011, **403**, 173-182.
81 J. M. Thomas, B. F. G. Johnson, R. Raja, G. Sankar and P. A. Midgley, *Accounts Chem. Res.*, 2003, **36**, 20-30.
82 S. Hermans, R. Raja, J. M. Thomas, B. F. G. Johnson, G. Sankar and D. Gleeson, *Angew. Chem. Int. Edit.*, 2001, **40**, 1211-1215.
83 S. U. Son, Y. Jang, J. Park, H. B. Na, H. M. Park, H. J. Yun, J. Lee and T. Hyeon, *J. Am. Chem. Soc.*, 2004, **126**, 5026-5027.
84 Y. Pan, F. Zhang, K. Wu, Z. Lu, Y. Chen, Y. Zhou, Y. Tang and T. Lu, *Int. J. Hydrogen Energ.*, 2012, **37**, 2993-3000.
85 T. I. Asanova, I. P. Asanov, M.-G. Kim, E. Y. Gerasimov, A. V. Zadesenets, P. E. Plyusnin and S. V. Korenev, *J. Nanopart. Res.*, 2013, **15**, 1994.
86 K. Ding, L. Liu, Y. Cao, X. Yan, H. Wei and Z. Guo, *Int. J. Hydrogen Energ.*, 2014, **39**, 7326-7337.
87 S. Sun, C. B. Murray, D. Weller, L. Folks and A. Moser, *Science*, 2000, **287**, 1989-1992.
88 R. Easterday, O. Sanchez-Felix, B. D. Stein, D. G. Morgan, M. Pink, Y. Losovyj and L. M. Bronstein, *J. Phys. Chem. C*, 2014, **118**, 24769-24775.
89 S. Song, R. Liu, Y. Zhang, J. Feng, D. Liu, Y. Xing, F. Zhao and H. Zhang, *Chem-Eur. J.*, 2010, **16**, 6251-6256.
90 Y. Shubin, P. Plyusnin and M. Sharafutdinov, *Nanotechnology*, 2012, **23**. 405302.
91 N. R. Kim, K. Shin, I. Jung, M. Shim and H. M. Lee, *J. Phys. Chem. C*, 2014, **118**, 26324-26331.
92 S. S. Shankar, A. Rai, B. Ankamwar, A. Singh, A. Ahmad and M. Sastry, *Nat. Mater.*, 2004, **3**, 482-488.
93 G. Zhan, J. Huang, M. Du, I. Abdul-Rauf, Y. Ma and Q. Li, *Mater. Lett.*, 2011, **65**, 2989-2991.
94 D. Sun, G. Zhang, X. Jiang, J. Huang, X. Jing, Y. Zheng, J. He and Q. Li, *J. Mater. Chem. A*, 2014, **2**, 1767-1773.
95 H. Liu, J. Huang, D. Sun, T. Odoom-Wubah, J. Li and Q. Li, *J. Nano. Res.*, 2014, **16**, 2698.
96 G. Zhang, M. Du, Q. Li, X. Li, J. Huang, X. Jiang and D. Sun, *RSC Adv.*, 2013, **3**, 1878-1884.
97 S. Mondal, N. Roy, R. A. Laskar, I. Sk, S. Basu, D. Mandal and N. A. Begum, *Colloid. Surface. B*, 2011, **82**, 497-504.
98 S. A. Dahoumane, K. Wijesekera, C. D. M. Filipe and J. D. Brennan, *J. Colloid Interf. Sci.*, 2014, **416**, 67-72.
99 S. S. Shankar, A. Rai, A. Ahmad and M. Sastry, *J. Colloid Interf. Sci.*, 2004, **275**, 496-502.
100 C. Tamuly, M. Hazarika, S. C. Borah, M. R. Das and M. P. Boruah, *Colloid. Surface. B*, 2013, **102**, 627-634.
101 S. Senapati, A. Ahmad, M. I. Khan, M. Sastry and R. Kumar, *Small*, 2005, **1**, 517-520.
102 Y. Zhang, G. Gao, Q. Qian and D. Cui, *Nanoscale Res. Le* 2012, **7**, 475.
103 E. Castro-Longoria, A. R. Vilchis-Nestor and M. Avalos-Borja *Colloid. Surface.*, 2011, **83**, 42-48.
104 J. M. Galloway and S. S. Staniland, *J. Mater. Chem.*, 2012, **2** 12423-12434.
105 K. N. L. Huggins, A. P. Schoen, M. A. Arunagirinathan and S. Heilshorn, *Adv. Funct. Mater.*, 2014, **24**, 7737-7744.
106 D. Raju, R. Mendapara and U. J. Mehta, *Mater. Lett.*, 201 **124**, 271-274.
107 R. M. Kramer, C. Li, D. C. Carter, M. O. Stone and R. R. Naik, *J. Am. Chem. Soc.*, 2004, **126**, 13282-13286.
108 H. Chen, D. Sun, X. Jiang, X. Jing, F. Lu, T. Odoom-Wubah, Zheng, J. Huang and Q. Li, *RSC Adv.*, 2013, **3**, 15389-15395.
109 I. Robinson, L. D. Tung, S. Maenosono, C. Waelti and N. T. K Thanh, *Nanoscale*, 2010, **2**, 2624-2630.
110 C. Zheng, A.-X. Zheng, B. Liu, X.-L. Zhang, Y. He, J. Li, H.-H. Y and G. Chen, *Chem. Commun.*, 2014, **50**, 13103-13106.
111 M. Fischler, U. Simon, H. Nir, Y. Eichen, G. A. Burley, J. Gier P. M. E. Gramlich and T. Carell, *Small*, 2007, **3**, 1049-1055.
112 S. Srivastava, B. Samanta, P. Arumugam, G. Han and V. Rotello, *J. Mater. Chem.*, 2007, **17**, 52-55.
113 C. B. Mao, D. J. Solis, B. D. Reiss, S. T. Kottmann, R. Y. Sweeney A. Hayhurst, G. Georgiou, B. Iverson and A. M. Belcher, *Science*, 2004, **303**, 213-217.
114 C. B. Mao, C. E. Flynn, A. Hayhurst, R. Sweeney, J. F. Qi, G Georgiou, B. Iverson and A. M. Belcher, *P. Natl Acad. Sci. USA* 2003, **100**, 6946-6951.
115 Y. J. Lee, Y. Lee, D. Oh, T. Chen, G. Ceder and A. M. Belcher *Nano Lett.*, 2010, **10**, 2433-2440.
116 K. T. Nam, D. W. Kim, P. J. Yoo, C. Y. Chiang, N. Meethong, P. Hammond, Y. M. Chiang and A. M. Belcher, *Science*, 2006, **312** 885-888.
117 Y. G. Sun, B. T. Mayers and Y. N. Xia, *Nano Lett.*, 2002, **2**, 481-485.
118 Y. Sun and C. Lei, *Angew. Chem. Int. Edit.*, 2009, **121**, 6956-6959.
119 Q. Jia, D. Zhao, B. Tang, N. Zhao, H. Li, Y. Sang, N. Bao, X Zhang, X. Xu and H. Liu, *J. Mater. Chem. A*, 2014, **2**, 16292 16298.
120 Y. Hu, Y. Liu, Z. Li and Y. Sun, *Adv. Funct. Mater.*, 2014, **24** 2828-2836.
121 H. Zhang, M. Jin, H. Liu, J. Wang, M. J. Kim, D. Yang, Z. Xie, J. Li and Y. Xia, *ACS Nano*, 2011, **5**, 8212-8222.
122 M. Tsuji, T. Kidera, A. Yajima, M. Hamasaki, M. Hattori, T. Tsuji and H. Kawazumi, *Crystengcomm*, 2014, **16**, 2684-2691.
123 H. Xu, B. W. Zeiger and K. S. Suslick, *Chem. Soc. Rev.*, 2013, **42** 2555-2567.
124 J. H. Bang and K. S. Suslick, *Adv. Mater.*, 2010, **22**, 1039-1059.
125 J. Zhang, J. Du, B. Han, Z. Liu, T. Jiang and Z. Zhang, *Angew Chem. Int. Edit.*, 2006, **45,** 1116-1119.
126 C.-H. Su, P.-L. Wu and C.-S. Yeh, *J. Phys. Chem. B*, 2003, **10** 14240-14243.
127 A. Nemamcha, J.-L. Rehspringer and D. Khatmi, *J. Phys. Chem B*, 2005, **110**, 383-387.

128 Y. Mizukoshi, T. Fujimoto, Y. Nagata, R. Oshima and Y. Maeda, *J. Phys. Chem. B*, 2000, **104**, 6028-6032.
129 Y. Mizukoshi, K. Okitsu, Y. Maeda, T. A. Yamamoto, R. Oshima and Y. Nagata, *J. Phys. Chem. B*, 1997, **101**, 7033-7037.
130 P. Estifaee, M. Haghighi, N. Mohammadi and F. Rahmani, *Ultrason. Sonochem.*, 2014, **21**, 1155-1165.
131 S. Anandan, A. Manivel and M. Ashokkumar, *Fuel Cells*, 2012, **12**, 956-962.
132 A. Shaabani and M. Mahyari, *J. Mater. Chem. A*, 2013, **1**, 9303-9311.
133 B. Neppolian, V. Sáez, J. González-García, F. Grieser, R. Gómez and M. Ashokkumar, *J. Solid State Electr.*, 2014, **18**, 3163-3171.
134 B. Neppolian, C. Wang and M. Ashokkumar, *Ultrason. Sonochem.*, 2014, **21**, 1948-1953.
135 H. Azizi-Toupkanloo, E. K. Goharshadi and P. Nancarrow, *Adv. Powder Technol.*, 2014, **25**, 801-810.
136 M. Treguer, C. de Cointet, H. Remita, J. Khatouri, M. Mostafavi, J. Amblard, J. Belloni and R. de Keyzer, *J. Phys. Chem. B*, 1998, **102**, 4310-4321.
137. A. L. Kovarskii, A. A. Revina, S. N. Dobryakov, L. M. Baider and N. A. Tikhonov, *Colloid J.*, 2004, **66**, 696-699.
138 C. M. Doudna, M. F. Bertino and A. T. Tokuhiro, *Langmuir*, 2002, **18**, 2434-2435.
139 S. Remita, M. Mostafavi and M. O. Delcourt, *Radiat. Phys. Chem.*, 1996, **47**, 275-279.
140 C. M. Doudna, M. F. Bertino, F. D. Blum, A. T. Tokuhiro, D. Lahiri-Dey, S. Chattopadhyay and J. Terry, *J. Phys. Chem. B*, 2003, **107**, 2966-2970.
141 M. Kumar, *Radiat. Phys. Chem.*, 2003, **66**, 403-409.
142 S. C. Tripathi and M. Kumar, *J. Radioanal. Nucl. Chem.*, 2003, **256**, 565-569.
143 S. Remita, M. Mostafavi and M. O. Delcourt, *Radiat. Phys. Chem.*, 1996, **47**, 275-279.
144 A. Sarkany, P. Hargittai and A. Horvath, *Top. Catal.*, 2007, **46**, 121-128.
145 A. Sárkány, P. Hargittai and O. Geszti, *Colloid. Surface. A.*, 2008, **322**, 124-129.
146 K. Roy and S. Lahiri, *Anal. Chem.*, 2008, **80**, 7504-7507.
147 M. Mirdamadi-Esfahani, M. Mostafavi, B. Keita, L. Nadjo, P. Kooyman and H. Remita, *Gold Bull.*, 2010, **43**, 49-56.
148 A. Abedini, F. Larki, E. B. Saion, A. Zakaria and M. Z. Hussein, *J. Radioanal. Nucl. Chem.*, 2012, **292**, 361-366.
149 B. Le Gratiet, H. Remita, G. Picq and M. O. Delcourt, *Radiat. Phys. Chem.*, 1996, **47**, 263-268.
150 S. E. Lohse and C. J. Murphy, *Chem. Mater.*, 2013, **25**, 1250-1261.
151 K. M. Mayer and J. H. Hafner, *Chem. Rev.*, 2011, **111**, 3828-3857.
152 J. Zhao, A. O. Pinchuk, J. M. McMahon, S. Li, L. K. Ausman, A. L. Atkinson and G. C. Schatz, *Accounts Chem. Res.*, 2008, **41**, 1710-1720.
153 I. Pastoriza-Santos and L. M. Liz-Marzán, *J. Mater. Chem.*, 2008, **18**, 1724-1737.
154 M. I. Mishchenko, L. D. Travis and A. A. Lacis, *Scattering, absorption, and emission of light by small particles*, Cambridge university press, U.K., 2002, ch. 5, pp. 116-119.
155 P. Nordlander, C. Oubre, E. Prodan, K. Li and M. I. Stockman, *Nano Lett.*, 2004, **4**, 899-903.
156 H. Wang, Y. Wu, B. Lassiter, C. L. Nehl, J. H. Hafner, P. Nordlander and N. J. Halas, *P. Natl Acad. Sci. USA*, 2006, **103**, 10856-10860.
157 M. Dridi and A. Vial, *J. Phys. Chem. C*, 2010, **114**, 9541-9545.
158 H. Tamaru, H. Kuwata, H. T. Miyazaki and K. Miyano, *Appl. Phys. Lett.*, 2002, **80**, 1826-1828.
159. S. Tanev, V. V. Tuchin and P. Paddon, *Laser Phys. Lett.*, 2006, **3**, 594-598.
160 J. Zhang, Y. Fu and F. Mandavi, *J. Phys. Chem. C*, 2012, **116**, 24224-24232.
161 Q. Zhang, D. Q. Lima, I. Lee, F. Zaera, M. F. Chi and Y. D. Yin, *Angew. Chem. Int. Edit.*, 2011, **50**, 7088-7092.
162 Y. Yang, Q. Zhang, Z.-W. Fu and D. Qin, *ACS Appl. Mater. Interf.*, 2014, **6**, 3750-3757.
163 S.-H. Ahn, D.-S. Kim, D. Seo, W. Choi, G.-R. Yi, H. Song, Q. H. Park and Z. H. Kim, *Phys. Chem. Chem. Phys.*, 2013, **15**, 4190-4194.
164 L.-C. Cheng, J.-H. Huang, H. M. Chen, T.-C. Lai, K.-Y. Yang, R.-S. Liu, M. Hsiao, C.-H. Chen, L.-J. Her and D. P. Tsai, *J. Mater. Chem.*, 2012, **22**, 2244-2253.
165 Y. Bu and S. Lee, *ACS Appl. Mater. Interf.*, 2012, **4**, 3923-3931.
166 H. He, X. Xu, H. Wu and Y. Jin, *Adv. Mater.*, 2012, **24**, 1730-1740.
167 X. Lopez-Lozano, C. Mottet and H. C. Weissker, *J. Phys. Chem. C*, 2013, **117**, 3062-3068.
168 R. Arenal, L. Henrard, L. Roiban, O. Ersen, J. Burgin and M. Treguer-Delapierre, *J. Phys. Chem. C*, 2014, **118**, 25643-25650.
169 K. Jia, M. Y. Khaywah, Y. Li, J. L. Bijeon, P. M. Adam, R. Deturche, B. Guelorget, M. Francois, G. Louarn and R. Ionescu, *ACS Appl. Mater. Interf.*, 2014, **6**, 219-227.
170 A. Kuzma, M. Weis, M. Daricek, J. Uhrik, F. Horinek, M. Donoval, F. Uherek and D. Donoval, *J. Appl. Phys.*, 2014, **115**, 053517.
171 P. N. Njoki, W. Wu, H. Zhao, L. Hutter, E. A. Schiff and M. M. Maye, *J. Am. Chem. Soc.*, 2011, **133**, 5224-5227.
172 P. N. Njoki, W. Wu, P. Lutz and M. M. Maye, *Chem. Mater.*, 2013, **25**, 3105-3113.
173 R. Singh and R. K. Soni, *Appl. Phys. A-Mater.*, 2014, **116**, 955-967.
174. A. Gopalakrishnan, M. Chirumamilla, F. De Angelis, A. Toma, P. P. Zaccaria and R. Krahne, *ACS Nano*, 2014, **8**, 7986-7994.
175 R. Jiang, F. Qin, Q. Ruan, J. Wang and C. Jin, *Adv. Funct. Mater.*, 2014, **24**, 7328-7337.
176 D. Ferrer, A. Torres-Castro, X. Gao, S. Sepulveda-Guzman, U. Ortiz-Mendez and M. Jose-Yacaman, *Nano Lett.*, 2007, **7**, 1701-1705.
177 R. Zhao, M. Gong, H. Zhu, Y. Chen, Y. Tang and T. Lu, *Nanoscale*, 2014, 6, 9273-9278.
178 C. Zhu, J. Zeng, J. Tao, M. C. Johnson, I. Schmidt-Krey, L. Blubaugh, Y. Zhu, Z. Gu and Y. Xia, *J. Am. Chem. Soc.*, 2012, **134**, 15822-15831.
179 E. Della Gaspera, M. Bersani, G. Mattei, N. Tich-Lam, P. Mulvaney and A. Martucci, *Nanoscale*, 2012, **4**, 5972-5979.
180 S. Chen, S. V. Jenkins, J. Tao, Y. Zhu and J. Chen, *J. Phys. Chem. C*, 2013, **117**, 8924-8932.

181 H. Jing, N. Large, Q. Zhang and H. Wang, *J. Phys. Chem. C*, 2014, **118**, 19948-19963.
182 Y.-H. Su and W.-L. Wang, *Nanoscale Res. Lett.*, 2013, **8**, 408.
183 H. She, Y. Chen, X. Chen, K. Zhang, Z. Wang and D.-L. Peng, *J. Mater. Chem.*, 2012, **22**, 2757-2765.
184 W. Li and F. Chen, *J. Nanopart. Res.*, 2013, **15**, 1809.
185 M. Jin, H. Zhang, J. Wang, X. Zhong, N. Lu, Z. Li, Z. Xie, M. J. Kim and Y. Xia, *ACS Nano*, 2012, **6**, 2566-2573.
186 M. Faustini, A. Capobianchi, G. Varvaro and D. Grosso, *Chem. Mater.*, 2012, **24**, 1072-1079.
187 S. Xie, N. Lu, Z. Xie, J. Wang, M. J. Kim and Y. Xia, *Angew. Chem. Int. Edit.*, 2012, **51**, 10266-10270.
188 T. Hyeon, *Chem. Commun.*, 2003, 927-934.
189 K.-M. Kang, H.-W. Kim, I.-W. Shim and H.-Y. Kwak, *Fuel Process. Technol.*, 2011, **92**, 1236-1243.
190 D. Kodama, K. Shinoda, K. Sato, Y. Konno, R. J. Joseyphus, K. Motomiya, H. Takahashi, T. Matsumoto, Y. Sato, K. Tohji and B. Jeyadevan, *Adv. Mater.*, 2006, **18**, 3154-3159.
191 F. Tao, M. E. Grass, Y. Zhang, D. R. Butcher, J. R. Renzas, Z. Liu, J. Y. Chung, B. S. Mun, M. Salmeron and G. A. Somorjai, *Science*, 2008, **322**, 932-934.
192 M. Mannini, F. Pineider, P. Sainctavit, C. Danieli, E. Otero, C. Sciancalepore, A. M. Talarico, M.-A. Arrio, A. Cornia, D. Gatteschi and R. Sessoli, *Nat. Mater.*, 2009, **8**, 194-197.
193 R. Mu, Q. Fu, H. Xu, H. Zhang, Y. Huang, Z. Jiang, S. Zhang, D. Tan and X. Bao, *J. Am. Chem. Soc.*, 2011, **133**, 1978-1986.
194 C. Binns, M. J. Maher, Q. A. Pankhurst, D. Kechrakos and K. N. Trohidou, *Phys. Rev. B*, 2002, **66**, 184413.
195 R. K. Kawakami, E. J. EscorciaAparicio and Z. Q. Qiu, *Phys. Rev. Lett.*, 1996, **77**, 2570-2573.
196 J. Li, A. Tan, K. W. Moon, A. Doran, M. A. Marcus, A. T. Young, E. Arenholz, S. Ma, R. F. Yang, C. Hwang and Z. Q. Qiu, *Appl. Phys. Lett.*, 2014, **104**, 112407.
197 K. Santhi, E. Thirumal, S. N. Karthick, H.-J. Kim, V. Narayanan and A. Stephen, *J. Alloy. Compd.*, 2013, **557**, 172-178.
198 S. J. Cho, A. M. Shahin, G. J. Long, J. E. Davies, K. Liu, F. Grandjean and S. M. Kauzlarich, *Chem. Mater.*, 2006, **18**, 960-967.
199 S. J. Cho, S. M. Kauzlarich, J. Olamit, K. Liu, F. Grandjean, L. Rebbouh and G. J. Long, *J. Appl. Phys.*, 2004, **95**, 6804-6806.
200 P. Ohresser, N. B. Brookes, S. Padovani, F. Scheurer and H. Bulou, *Phys. Rev. B*, 2001, **64**, 104429.
201 L. F. Kiss, D. Kaptás, J. Balogh, F. Tanczikó, M. Major and I. Vincze, *J. Alloy. Compd.*, 2009, **483**, 620-622.
202 K. Santhi, E. Thirumal, S. N. Karthick, H.-J. Kim, V. Narayanan and A. Stephen, *J. Alloy. Compd.*, 2013, **557**, 172-178.
203 J. Alonso, M. L. Fdez-Gubieda, G. Sarmiento, J. Chaboy, R. Boada, A. Garcia Prieto, D. Haskel, M. A. Laguna-Marco, J. C. Lang, C. Meneghini, L. Fernandez Barquin, T. Neisius and I. Orue, *Nanotechnology*, 2012, **23**, 025705.
204 J. Alonso, M. L. Fdez-Gubieda, A. Svalov, C. Meneghini and I. Orue, *J. Alloy. Compd.*, 2012, 536, **Supplement 1**, S271-S276.
205 W. Zhang, D. Ma, Y. Li, K. Yubuta, X. Liang and D. Peng, *J. Alloy. Compd.*, 2014, 615, **Supplement 1**, S252-S255.
206 J. U. Thiele, K. R. Coffey, M. F. Toney, J. A. Hedstrom and A. J. Kellock, *J. Appl. Phys.*, 2002, **91**, 6595-6600.
207 J. Kudrnovsky, V. Drchal, S. Khmelevskyi and I. Turek, *Phys. Rev. B*, 2011, **84**, 214436.
208 Y. Ito, A. Miyazaki, S. Valiyaveettil and T. Enoki, *J. Phys. Che C*, 2010, **114**, 11699-11702.
209 C. d. J. Fernández, G. Mattei, E. Paz, R. L. Novak, L. Cavigli, Bogani, F. J. Palomares, P. Mazzoldi and A. Caneschi *Nanotechnology*, 2010, **21**, 165701.
210 P. Mukherjee, P. Manchanda, P. Kumar, L. Zhou, M. J. Kramer, A. Kashyap, R. Skomski, D. Sellmyer and J. E. Shield, *ACS Nan* , 2014, **8**, 8113-8120.
211 K. Santhi, E. Thirumal, S. N. Karthick, H.-J. Kim, M. Nidhin, Narayanan and A. Stephen, *J. Nanopart. Res.*, 2012, **14**, 868.
212 H. Hori, T. Teranishi, M. Taki, S. Yamada, M. Miyake and Y. Yamamoto, *J. Magn. Magn. Mater.*, 2001, **226**, 1910-1911.
213 P. K. Sahoo, B. Panigrahy and D. Bahadur, *RSC Adv.*, 2014, , 48563-48571.
214 Y. Zhang, M. DaSilva, B. Ashall, G. Doyle, D. Zerulla, T. D. Sand and G. U. Lee, *Langmuir*, 2011, **27**, 15292-15298.
215 T.-R. Ger, H.-T. Huang, C.-Y. Huang, W.-C. Liu, J.-Y. Lai, B.-T. J.-Y. Chen, C.-W. Hong, P.-J. Chen and M.-F. Lai, *J. Appl. Phys.*, 2014, **115**, 17B528.
216 S. Senapati, S. K. Srivastava, S. B. Singh and H. N. Mishra, *J. Mater. Chem.*, 2012, **22**, 6899-6906.
217 C. C. Lee and D. H. Chen, *Nanotechnology*, 2006, **17**, 3094 3099.
218 M. B. Gawande, A. K. Rathi, J. Tucek, K. Safarova, M Bundaleski, O. M. N. D. Teodoro, L. Kvitek, R. S. Varma and Zboril, *Green Chem.*, 2014, **16**, 4137-4143.
219 V. Mathet, T. Devolder, C. Chappert, J. Ferre, S. Lemerle, Belliard and G. Guentherodt, *J. Magn. Magn. Mater.*, 2003, **260**, 295-304.
220 S. Oikawa, A. Shibata, S. Iwata and S. Tsunashima, *J. Magn. Magn. Mater.*, 1998, **177**, 1273-1274.
221 C. Train, R. Megy and C. Chappert, *J. Magn. Magn. Mater.*, 1999, **202**, 321-326.
222 X. Chen, G. Wu, J. Chen, X. Chen, Z. Xie and X. Wang, *J. Am. Chem. Soc.*, 2011, **133**, 3693-3695.
223 S. Kidambi, J. H. Dai, J. Li and M. L. Bruening, *J. Am. Chem. Soc.*, 2004, **126**, 2658-2659.
224 V. Mazumder and S. Sun, *J. Am. Chem. Soc.*, 2009, **131**, 4588 4589.
225 W. Yu, M. D. Porosoff and J. G. Chen, *Chem. Rev.*, 2012, 5780-5817.
226 X. Liu, D. Wang and Y. Li, *Nano Today*, 2012, **7**, 448-466.
227 H. Zhang, M. Jin and Y. Xia, *Chem. Soc. Rev.*, 2012, **41**, 8035 8049.
228 L. Zhang, S.-I. Choi, J. Tao, H.-C. Peng, S. Xie, Y. Zhu, Z. Xie and Y. Xia, *Adv. Funct. Mater.*, 2014, **24**, 7520-7529.
229 Z.-Q. Zhang, J. Huang, L. Zhang, M. Sun, Y.-C. Wang, Y. Lin and J. Zeng, *Nanotechnology*, 2014, **25**, 435602.
230 D. J. Childers, N. M. Schweitzer, S. M. K. Shahari, R. M. Rioux, J. T. Miller and R. J. Meyer, *J. Catal.*, 2014, **318**, 75-84.
231 A. Bonilla Sanchez, N. Homs, S. Miachon, J.-A. Dalmon, J. L. G. Fierro and P. Ramirez de la Piscina, *Green Chem.*, 2011, **1** , 2569-2575.
232 W. E. Kaden, T. Wu, W. A. Kunkel and S. L. Anderson, *Science* 2009, **326**, 826-829.

233 M. Scott, M. Goeffroy, W. Chiu, M. A. Blackford and H. Idriss, *Top. Catal.*, 2008, **51**, 13-21.
234 J.-N. Park and E. W. McFarland, *J. Catal.*, 2009, **266**, 92-97.
235 S. Sitthisa, P. Trung, T. Prasomsri, T. Sooknoi, R. G. Mallinson and D. E. Resasco, *J. Catal.*, 2011, **280**, 17-27.
236 Q. Zhang, I. Lee, J. P. Ge, F. Zaera and Y. D. Yin, *Adv. Funct. Mater.*, 2010, **20**, 2201-2214.
237 X.-B. Zhang, J.-M. Yan, S. Han, H. Shioyama and Q. Xu, *J. Am. Chem. Soc.*, 2009, **131**, 2778-2779.
238 J.-M. Yan, X.-B. Zhang, T. Akita, M. Haruta and Q. Xu, *J. Am. Chem. Soc.*, 2010, **132**, 5326-5327.
239 D.-H. Zhang, G.-D. Li, J.-X. Li and J.-S. Chen, *Chem. Commun.*, 2008, 3414-3416.
240 M. Zhu and G. Diao, *J. Phys. Chem. C*, 2011, **115**, 24743-24749.
241 Y. Jang, J. Chung, S. Kim, S. W. Jun, B. H. Kim, D. W. Lee, B. M. Kim and T. Hyeon, *Phys. Chem. Chem. Phys.*, 2011, **13**, 2512-2516.
242 Y. Jang, S. Kim, S. W. Jun, B. H. Kim, S. Hwang, I. K. Song, B. M. Kim and T. Hyeon, *Chem. Commun.*, 2011, **47**, 3601-3603.
243 J. Wang, Y.-L. Qin, X. Liu and X.-B. Zhang, *J. Mater. Chem.*, 2012, **22**, 12468-12470.
244 B. Lim, M. Jiang, P. H. C. Camargo, E. C. Cho, J. Tao, X. Lu, Y. Zhu and Y. Xia, *Science*, 2009, **324**, 1302-1305.
245 C. Koenigsmann, A. C. Santulli, K. Gong, M. B. Vukmirovic, W.-p. Zhou, E. Sutter, S. S. Wong and R. R. Adzic, *J. Am. Chem. Soc.*, 2011, **133**, 9783-9795.
246 M. Shao, K. Shoemaker, A. Peles, K. Kaneko and L. Protsailo, *J. Am. Chem. Soc.*, 2010, **132**, 9253-9255.
247 J. W. Hong, S. W. Kang, B.-S. Choi, D. Kim, S. B. Lee and S. W. Han, *ACS Nano*, 2012, **6**, 2410-2419.
248 A.-X. Yin, X.-Q. Min, Y.-W. Zhang and C.-H. Yan, *J. Am. Chem. Soc.*,, 2011, **133**, 3816-3819.
249 J. Hermannsdoerfer, M. Friedrich, N. Miyajima, R. Q. Albuquerque, S. Kuemmel and R. Kempe, *Angew. Chem. Int. Edit.*, 2012, **51**, 11473-11477.
250 Y. Imura, K. Tsujimoto, C. Morita and T. Kawai, *Langmuir*, 2014, **30**, 5026-5030.
251 S. Takenaka, Y. Shigeta, E. Tanabe and K. Otsuka, *J. Catal.*, 2003, **220**, 468-477.
252 S. Li, D. Cheng, X. Qiu and D. Cao, *Electrochim. Acta*, 2014, **143**, 44-48.
253 A. J. McCue, C. J. McRitchie, A. M. Shepherd and J. A. Anderson, *J. Catal.*, 2014, **319**, 127-135.
254 W. Xu, H. Sun, B. Yu, G. Zhang, W. Zhang and Z. Gao, *ACS Appl. Mater. Interf.*, 2014, **6**, 20261-20268.
255 D. Cheng, H. Xu and A. Fortunelli, *J. Catal.*, 2014, **314**, 47-55.
256 J. Son, S. Cho, C. Lee, Y. Lee and J. H. Shim, *Langmuir*, 2014, **30**, 3579-3588.
257 W.-Y. Yu, G. M. Mullen, D. W. Flaherty and C. B. Mullins, *J. Am. Chem. Soc.*, 2014, **136**, 11070-11078.
258 Y. Feng, H. Yin, D. Gao, A. Wang, L. Shen and M. Meng, *J. Catal.*, 2014, **316**, 67-77.
259 J. Suntivich, Z. Xu, C. E. Carlton, J. Kim, B. Han, S. W. Lee, N. Bonnet, N. Marzari, L. F. Allard, H. A. Gasteiger, K. Hamad-Schifferli and Y. Shao-Horn, *J. Am. Chem. Soc.*, 2013, **135**, 7985-7991.
260 Y. Yu, K. H. Lim, J. Y. Wang and X. Wang, *J. Phys. Chem. C*, 2011, **116**, 3851-3856.
261 H. M. Song, D. H. Anjum, R. Sougrat, M. N. Hedhili and N. [illegible] Khashab, *J. Mater. Chem.*, 2012, **22**, 25003-25010.
262 C.-W. Liu, Y.-C. Wei, C.-C. Liu and K.-W. Wang, *J. Mater. Chem.*, 2012, **22**, 4641-4644.
263 X. Zhong, H. Yu, X. Wang, L. Liu, Y. Jiang, L. Wang, G. Zhuang, [illegible] Chu, X. Li and J.-G. Wang, *ACS Appl. Mater. Interf.*, 2014, **6**, 13448-13454.
264 T. Kaito, H. Mitsumoto, S. Sugawara, K. Shinohara, H. Uehara, H. Ariga, S. Takakusagi, Y. Hatakeyama, K. Nishikawa and [illegible] Asakura, *J. Phys. Chem. C*, 2014, **118**, 8481-8490.
265 Y. Wei, Z. Zhao, J. Liu, S. Liu, C. Xu, A. Duan and G. Jiang, *J. Catal.*, 2014, **317**, 62-74.
266 E. S. Steigerwalt, G. A. Deluga, D. E. Cliffel and C. M. Lukehart, *J. Phys. Chem. B*, 2001, **105**, 8097-8101.
267 E. S. Steigerwalt, G. A. Deluga and C. M. Lukehart, *J. Phys. Chem. B*, 2002, **106**, 760-766.
268 N. Kakati, J. Maiti, S. H. Lee, S. H. Jee, B. Viswanathan and [illegible] Yoon, *Chem. Rev.*, 2014, **114**, 12397-12429.
269 S. Alayoglu, A. U. Nilekar, M. Mavrikakis and B. Eichhorn, *[illegible] Mater.*, 2008, **7**, 333-338.
270 Tong, H. S. Kim, P. K. Babu, P. Waszczuk, A. Wieckowski and [illegible] Oldfield, *J. Am. Chem. Soc.*, 2001, **124**, 468-473.
271 N. Muthuswamy, J. L. G. de la Fuente, D. T. Tran, J. Walmsley, M. Tsypkin, S. Raaen, S. Sunde, M. Rønning and D. Chen, *Int. J. Hydrogen Energ.*, 2013, **38**, 16631-16641.
272 A.-C. Johansson, J. V. Larsen, M. A. Verheijen, K. B. Haugshøj, H. F. Clausen, W. M. M. Kessels, L. H. Christensen and E. [illegible] Thomsen, *J. Catal.*, 2014, **311**, 481-486.
273 H.-L. Jiang, T. Umegaki, T. Akita, X.-B. Zhang, M. Haruta and [illegible] Xu, *Chem-Eur. J.*, 2010, **16**, 3132-3137.
274 J. Knudsen, L. R. Merte, G. Peng, R. T. Vang, A. Resta, [illegible] Lægsgaard, J. N. Andersen, M. Mavrikakis and F. Besenbacher, *ACS Nano*, 2010, **4**, 4380-4387.
275 G. Yuan, C. Louis, L. Delannoy and M. A. Keane, *J. Catal.*, 2007, **247**, 256-268.
276 A. M. Molenbroek, J. K. Nørskov and B. S. Clausen, *J. Phys. Chem. B*, 2001, **105**, 5450-5458.
277 Y.-H. Chin, D. L. King, H.-S. Roh, Y. Wang and S. M. Heald, *J. Catal.*, 2006, **244**, 153-162.
278 H. Nishikawa, D. Kawamoto, Y. Yamamoto, T. Ishida, H. Ohashi, T. Akita, T. Honma, H. Oji, Y. Kobayashi, A. Hamasaki, T. Yokoyama and M. Tokunaga, *J. Catal.*, 2013, **307**, 254-264.
279 Y.-W. Lee and K.-W. Park, *Catal. Commun.*, 2014, **55**, 24-28.
280 Q. Zheng, C. Janke and R. Farrauto, *Appl. Catal. B-Environ.*, 2014, **160-161**, 525-533.
281 H. B. Zhu, D. H. Anjum, Q. X. Wang, E. Abou-Hamad, L. Emsley, H. L. Dong, P. Laveille, L. D. Li, A. K. Samal and J. M. Basset, *J. Catal.*, 2014, **320**, 52-62.
282 Y. Zhang, Y. Zhou, J. Shi, S. Zhou, X. Sheng, Z. Zhang and S. Xiang, *J. Mol. Catal. A-Chem.*, 2014, **381**, 138-147.
283 A. Holewinski, J.-C. Idrobo and S. Linic, *Nat. Chem.*, 2014, **6**, 828-834.
284 J. J. H. B. Sattler, I. D. Gonzalez-Jimenez, L. Luo, B. A. Stears, A. Malek, D. G. Barton, B. A. Kilos, M. P. Kaminsky, T. W. G. M.

Verhoeven, E. J. Koers, M. Baldus and B. M. Weckhuysen, *Angew. Chem. Int. Ed.*, 2014, **53**, 9251-9256.
285 P. Sun, G. Siddiqi, M. Chi and A. T. Bell, *J. Catal.*, 2010, **274**, 192-199.
286 G. Siddiqi, P. Sun, V. Galvita and A. T. Bell, *J. Catal.*, 2010, **274**, 200-206.
287 L.-X. Ding, A.-L. Wang, Y.-N. Ou, Q. Li, R. Guo, W.-X. Zhao, Y.-X. Tong and G.-R. Li, *Sci. Rep.*, 2013, **3**, 1181.
288 A. O. Costa, L. S. Ferreira, F. B. Passos, M. P. Maia and F. C. Peixoto, *Appl. Catal. A-Gen.*, 2012, **445-446**, 26-34.
289 Y. Matsumura, *Appl. Catal. A-Gen.*, 2013, **468**, 350-358.
290 K. Foettinger and G. Rupprechter, *Accounts Chem. Res.*, 2014, **47**, 3071-3079.
291 X. Xu, X. Zhang, H. Sun, Y. Yang, X. Dai, J. Gao, X. Li, P. Zhang, H.-H. Wang, N.-F. Yu and S.-G. Sun, *Angew. Chem. Int. Edit.*, 2014, **53**, 12522-12527.
292 A. Tomita, K.-i. Shimizu, K. Kato, T. Akita and Y. Tai, *J. Phys. Chem. C*, 2013, **117**, 1268-1277.
293 Y.-H. Zhao, M.-M. Yang, D. Sun, H.-Y. Su, K. Sun, X. Ma, X. Bao and W.-X. Li, *J. Phys. Chem. C*, 2011, **115**, 18247-18256.
294 A. B. Hungria, R. Raja, R. D. Adams, B. Captain, J. M. Thomas, P. A. Midgley, V. Golovko and B. F. G. Johnson, *Angew. Chem. Int. Edit.*, 2006, **45**, 4782-4785.
295 Y. Wu, D. Wang, X. Chen, G. Zhou, R. Yu and Y. Li, *J. Am. Chem. Soc.*, 2013, **135**, 12220-12223.
296 L. Wang and Y. Yamauchi, *Chem. Mater.*, 2011, **23**, 2457-2465.
297 G.-R. Zhang, J. Wu and B.-Q. Xu, *J. Phys. Chem. C*, 2012, **116**, 20839-20847.
298 D. Wang, H. L. Xin, Y. Yu, H. Wang, E. Rus, D. A. Muller and H. D. Abruna, *J. Am. Chem. Soc.*, 2010, **132**, 17664-17666.
299 D. Wang, H. L. Xin, H. Wang, Y. Yu, E. Rus, D. A. Muller, F. J. DiSalvo and H. D. Abruna, *Chem. Mater.*, 2012, **24**, 2274-2281.
300 T. Cochell and A. Manthiram, *Langmuir*, 2012, **28**, 1579-1587.
301 S.-I. Choi, M. Shao, N. Lu, A. Ruditskiy, H.-C. Peng, J. Park, S. Guerrero, J. Wang, M. J. Kim and Y. Xia, *ACS Nano*, 2014, **8**, 10363-10371.
302 V. R. Stamenkovic, B. S. Mun, M. Arenz, K. J. J. Mayrhofer, C. A. Lucas, G. Wang, P. N. Ross and N. M. Markovic, *Nat. Mater.*, 2007, **6**, 241-247.
303 J. Greeley, I. E. L. Stephens, A. S. Bondarenko, T. P. Johansson, H. A. Hansen, T. F. Jaramillo, J. Rossmeisl, I. Chorkendorff and J. K. Norskov, *Nat. Chem.*, 2009, **1**, 552-556.
304 X. Liu, G. Fu, Y. Chen, Y. Tang, P. She and T. Lu, *Chem-Eur. J.*, 2014, **20**, 585-590.
305 D. Wang, H. L. Xin, Y. Yu, H. Wang, E. Rus, D. A. Muller and H. D. Abruña, *J. Am. Chem. Soc.*, 2010, **132**, 17664-17666.
306 S. Guo, X. Zhang, W. Zhu, K. He, D. Su, A. Mendoza-Garcia, S. F. Ho, G. Lu and S. Sun, *J. Am. Chem. Soc.*, 2014, **136**, 15026-15033.
307 K. Yang, J. Liu, R. Si, X. Chen, W. Dai and X. Fu, *J. Catal.*, 2014, **317**, 229-239.
308 D. Widmann, E. Hocking and R. J. Behm, *J. Catal.*, 2014, **317**, 272-276.
309 C. Han, X. Yang, G. Gao, J. Wang, H. Lu, J. Liu, M. Tong and X. Liang, *Green Chem.*, 2014, **16**, 3603-3615.
310 E. Taboada, I. Angurell and J. Llorca, *J. Catal.*, 2014, **309**, 460-467.
311 D. Ding, K. Liu, S. He, C. Gao and Y. Yin, *Nano Lett.*, 2014, **14**, 6731-6736.
312 J. Saavedra, C. Powell, B. Panthi, C. J. Pursell and B. Chandler, *J. Catal.*, 2013, **307**, 37-47.
313 I. X. Green, W. Tang, M. Neurock and J. T. Yates, *Accounts Chem. Res.*, 2013, **47**, 805-815.
314 M. Du, D. Sun, H. Yang, J. Huang, X. Jing, T. Odoom-Wubah, J. Wang, L. Jia and Q. Li, *J. Phys. Chem. C*, 2014, **118**, 19150-19157.
315 A. V. Puga, A. Forneli, H. García and A. Corma, *Adv. Funct. Mater.*, 2014, **24**, 241-248.
316 M. McEntee, W. Tang, M. Neurock and J. T. Yates, *J. Am. Chem. Soc.*, 2014, **136**, 5116-5120.
317 G. Schubert, A. Gazsi and F. Solymosi, *J. Catal.*, 2014, **313**, 127-134.
318 Y.-G. Wang, Y. Yoon, V.-A. Glezakou, J. Li and R. Rousseau, *J. Am. Chem. Soc.*, 2013, **135**, 10673-10683.
319 S. Hong and T. S. Rahman, *J. Am. Chem. Soc.*, 2013, **135**, 7629-7635.
320 L. Li and X. C. Zeng, *J. Am. Chem. Soc.*, 2014, **136**, 15857-15860.
321 Y. Guan, N. Zhao, B. Tang, Q. Jia, X. Xu, H. Liu and F. Boughton, *Chem. Commun.*, 2013, **49**, 11524-11526.
322 A. Sandoval, A. Aguilar, C. Louis, A. Traverse and R. Zanella, *J. Catal.*, 2011, **281**, 40-49.
323 P. Kundu, N. Singhania, G. Madras and N. Ravishankar, *Dalton T.*, 2012, **41**, 8762-8766.
324 S. Dulnee, A. Luengnaruemitchai and R. Wanchanthuek, *Int. Hydrogen Energ.*, 2014, **39**, 6443-6453.
325 H. Noei, A. Birkner, K. Merz, M. Muhler and Y. Wang, *J. Phys. Chemistry C*, 2012, **116,** 11181-11188.
326 N. Guo, R. Lu, S. Liu, G. W. Ho and C. Zhang, *J. Phys. Chemist. C*, 2014, **118**, 21038-21041.
327 M. Misra, P. Kapur and M. L. Singla, *Appl. Cataly. B-Enviro.*, 2014, **150-151**, 605-611.
328. C. Wang, O. Ranasingha, S. Natesakhawat, P. R. Ohodnicki, Jr., M. Andio, J. P. Lewis and C. Matranga, *Nanoscale*, 2013, **5**, 6968-6974.
329 P. Christopher and S. Linic, *J. Am. Chem. Soc.*, 2008, **130**, 11264-11265.
330 P. Christopher, H. Xin and S. Linic, *Nat. Chem.,* 2011, **3**, 467-472.
331 P. Christopher, H. Xin, A. Marimuthu and S. Linic, *Nat. Mat.*, 2012, **11**, 1044-1050.
332 A. Wittstock, V. Zielasek, J. Biener, C. M. Friend and M. Bäumer, *Science*, 2010, ***327,*** 319-322.
333 Y. Lei, F. Mehmood, S. Lee, J. Greeley, B. Lee, S. Seifert, R. E. Winans, J. W. Elam, R. J. Meyer and P. C. Redfern, *Science*, 2010, **328**, 224-228.
334 U. K. Singh and M. Albert Vannice, *J. Catal.*, 2000, **191**, 165-180.
335 S. Mukherjee and M. A. Vannice, *J. Catal.*, 2006, **243**, 108-130.
336 J. M. Krier, W. D. Michalak, X. Cai, L. Carl, K. Komvopoulos and G. A. Somorjai, *Nano Lett., 2015,* **15**, 39-44.
337 L. Shang, T. Bian, B. Zhang, D. Zhang, L. Z. Wu, C. H. Tung, Y. Yin and T. Zhang, *Angew. Chem. Int. Edit.*, 2014, **126**, 254-258.
338 M. F. Camellone nd S. Fabris, *J. Am. Chem. Soc.*, 2009, **131**, 10473-10483.

339 H. Y. Kim, H. M. Lee and G. Henkelman, *J. Am. Chem. Soc.*, 2011, **134**, 1560-1570.

Biography

Dr. Yong Xu obtained his PhD degree in Chemical Physics from University of Science and Technology in 2013 under the supervision of Professor Quanxin Li. From 2011 to 2012, he was a joint PhD student at Laboratori Nazionali di Frascati, Istituto Nazionale Di Fisica Nucleare (LNF-INFN), Italy, under the supervision of Professor A. Marcelli. He joined Shanghai Advanced Research Institute, Chinese Academy of Sciences (SARI-CAS), as an assistant researcher in 2013. Now he is a postdoctoral fellow in the college of Nano Science and Technology at Soochow University, working with Professor Qiao Zhang. His current research interest focuses on the synthesis and catalytic application of noble metal nanomaterials.

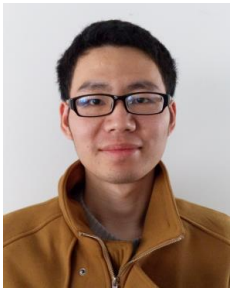

Lei Chen was born in Jiangsu, China, in 1992. He obtained his B.S. degree in Polymer Materials and Engineering from Soochow University in 2014. Now he is a graduate student at Soochow University under supervision of Professor Qiao Zhang. His current research interest focuses on the synthesis of noble metal nanoparticles and their application in catalysis.

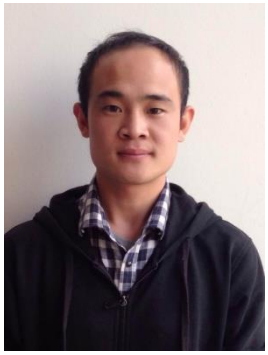

Xuchun Wang was born in Shandong, China, in 1990. He obtained his B.S. Degree in Chemistry from Soochow University in 2014. Now he is a graduate student at Soochow University under the supervision of Professor Qiao Zhang. His current research interest focuses on the colloidal synthesis and catalytic applications of noble metal nanoparticles.

Dr. Wei-Tang Yao obtained his PhD degree in Inorganic Chemistry from University of Science and Technology of China in 2005 under the supervision of Professor Shu-Hong Yu. He was a postdoctoral fellow in the Division of Nanomaterials and Chemistry at Hefei National Laboratory for Physical Sciences at the Microscale from 2005 to 2007. He was a postdoctoral fellow at the Max Planck Institute of Colloids and Interfaces, Germany, working with Dr. Cristina Giordano and Prof. Markus Antonietti (2008-2009). From 2009 to 2010, he joined Domen-Kubota Lab, University of Tokyo, as a Postdoctoral Researcher. From 2010 to 2014, he was appointed as an associate professor in the Department of New Energy, Hefei University of Technology. Since 2015, He became a faculty member of Southwest University of Science and Technology. His current research interest focuses on the studies of II-VI semiconductor nanomaterials, hybrid materials, functional metal nitrides, and conducting rubber ambers, and their related properties.

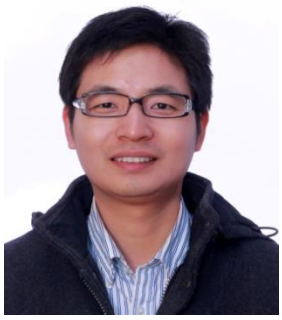

Dr. Qiao Zhang received his Ph.D. in physical chemistry from the University of California, Riverside, in 2012 under the supervision of Prof. Yadong Yin, then worked as a postdoctoral fellow at the University of California, Berkeley and the Lawrence Berkeley National Laboratory, under the supervision of Prof. A. Paul Alivisatos and Prof. Gabor A. Somorjai. In 2014, he became a faculty member of Soochow University. His research interests include synthesis and utilization of nanostructured materials for applications in fields such as catalysis, photonics, and biomedical research.